Hsp90 function by its cochaperone activity (11). However, the roles of hB-ind1 in the life cycle of HCV have not been precisely clarified. In this study, we investigated the role of the Hsp90-related chaperone system, including hB-ind1, in the regulation of the RNA replication and particle production of HCV.

MATERIALS AND METHODS

Plasmids. The plasmids encoding hB-ind1, NS5A, Hsp90, and FK506-binding protein 8 (FKBP8) were prepared by methods described previously (45, 56). The DNA fragments encoding hB-ind1 mutants were prepared by PCR with the introduction of a silent mutation that is resistant to the short hairpin RNA in the hB-ind1 knockdown cells, as described previously (56). The human p23 gene and glucose-regulated protein 78 (GRP78) promoter region (−151 to +22) were amplified by PCR from the total cDNA and genomic DNA of Huh7 cells, respectively. The DNA fragments encoding mutants of hB-ind1 and p23 were prepared by the method of splicing by overlap extension (26) and introduced into pEF FLAGGs pGKpuro (28). The GRP78 promoter region was introduced between the KpnI and HindIII sites of pGL3-basic (Promega, Madison, WI) and designated pGRP78-luc. The reporter plasmid carrying a firefly luciferase gene under the control of the GR promoter (pGR-luc) was purchased from Panomics (Fremont, CA). The internal-control plasmid encoding a *Renilla* luciferase (pRL-TK) was purchased from Promega. The plasmid pFK-I_{389} neo/NS3-3′/NK5.1 (47) was kindly provided by R. Bartenschlager. The plasmids used in this study were confirmed by sequencing them with an ABI Prism 3130 genetic analyzer (Applied Biosystems, Tokyo, Japan).

Cells and virus infection. All cell lines were cultured at 37°C under a humidified atmosphere and 5% CO_2. The human embryonic kidney 293T and hepatocellular carcinoma Huh7 cell lines were maintained in Dulbecco's modified Eagle's medium (DMEM) (Sigma, St. Louis, MO) supplemented with 100 U/ml penicillin, 100 μg/ml streptomycin, and 10% fetal calf serum (FCS). The human hepatocellular carcinoma cell line Huh7.5.1 was kindly provided by F. Chisari (70) and was maintained in DMEM containing nonessential amino acids, 100 U/ml penicillin, 100 μg/ml streptomycin, and 10% FCS. The Huh9-13 cell line, which is a Huh7 cell line harboring a subgenomic HCV RNA replicon (35), was maintained in DMEM containing 10% FCS, nonessential amino acids, and 1 mg/ml G418 (Nakalai Tesque, Kyoto, Japan). The hB-ind1 knockdown cell line Huh-KD and control cell line Huh-ctrl were described previously (56). Huh-KD cells were transfected with each of the expression plasmids encoding wild-type or mutant hB-ind1 and cultured for 1 week in the presence of 10 μg/ml of puromycin. The remaining cells were used for the experiments described below. The viral RNA of JFH1 was introduced into Huh7.5.1 cells according to the method of Wakita et al. (62) for preparation of the infectious HCV particles in cell culture.

Antibodies. The rabbit anti-hB-ind1 antibody was prepared as described previously (56). Mouse monoclonal antibodies to HCV NS5A, influenza virus hemagglutinin (HA) and FLAG tags, and β-actin were purchased from Austral Biologicals (San Ramon, CA), Covance (Richmond, CA), and Sigma, respectively. Mouse anti-protein disulfide isomerase (PDI) immunoglobulin G2a (IgG2a) was from Affinity Bioreagents (Golden, CO). Mouse anti-double-stranded RNA (dsRNA) IgG2a (J1 and K2) antibodies were from Biocenter Ltd. (Szirak, Hungary). Alexa Fluor 488 (AF488)-conjugated anti-mouse IgG1, AF647-conjugated anti-rabbit IgG, and AF594-conjugated anti-mouse IgG2a and IgG2b antibodies were from Invitrogen (San Diego, CA).

Transfection, immunoblotting, and immunoprecipitation. Transfection and immunoprecipitation analyses were carried out as described previously (25, 45). Immunoprecipitates boiled in loading buffer were subjected to 12.5% sodium dodecyl sulfate-polyacrylamide gel electrophoresis. The proteins were transferred to polyvinylidene difluoride membranes (Millipore, Bedford, MA) and were reacted with the appropriate antibodies. The immune complexes were visualized with Super Signal West Femto substrate (Pierce, Rockford, IL) and detected by an LAS-3000 image analyzer system (Fujifilm, Tokyo, Japan). The protein bands of GRP78 and β-actin were quantified by Multi Gauge software (Fujifilm), and the values of GRP78 expression were normalized with those of β-actin.

Quantitative reverse transcriptase PCR. HCV RNA was estimated by the method described previously (56). Total RNA was prepared from cells by using an RNeasy minikit (Qiagen, Tokyo, Japan). First-strand cDNA was synthesized using an RNA LA PCR in vitro cloning kit (Takara Bio Inc., Shiga, Japan) and random primers. Each cDNA was estimated with Platinum SYBR green qPCR SuperMix UDG (Invitrogen) according to the manufacturer's protocol. Fluorescent signals were analyzed with an ABI Prism 7000 (Applied Biosystems). The internal ribosomal entry site regions of HCV and mRNAs of GAPDH (glyceraldehyde-3-phosphate dehydrogenase), GRP78, and growth arrest- and DNA damage-inducible gene 153 (GADD153) were amplified using the primer pairs 5′-GAGTGTCGTGCAGCCTCCA-3′ and 5′-CACTCGCAAGCACCCTATCA-3′, 5′-GAAGGTGAAGGTCGGAGTC-3′ and 5′-GAAGGTGAAGGTCGGAGTC-3′, 5′-CGCCAAGCGGCTCATC-3′ and 5′-AACCACCTTGAACGGCAAGA-3′, and 5′-AGCTGGAACCTGAGGAGAGA-3′ and 5′-TGGATCAGTCTGGAAAAGCA-3′, respectively. The values of the HCV genome or each mRNA were normalized with those of GAPDH mRNA. Each PCR product was detected as a single band of the correct size on agarose gel electrophoresis (data not shown).

In vitro transcription and RNA transfection. The plasmid pFK-I_{389} neo/NS3-3′/NK5.1 was linearized by treatment with ScaI and then transcribed in vitro using the MEGAscript T7 kit (Applied Biosystems) according to the manufacturer's protocol. The in vitro-transcribed RNA was electroporated into cells at 4 million cells/0.4 ml under conditions of 270 V and 960 μF using a Gene Pulser (Bio-Rad, Hercules, CA). The colony formation assay was carried out by a method described previously (45).

Indirect immunofluorescence assay. Cells cultured on glass slides were fixed with 4% paraformaldehyde in phosphate-buffered saline (PBS) at room temperature for 30 min. After being washed twice with PBS, the cells were permeabilized for 20 min at room temperature with PBS containing 0.25% saponin and blocked with PBS containing 0.2% gelatin (gelatin-PBS) for 60 min at room temperature. The cells were incubated with gelatin-PBS containing rabbit anti-hB-ind1 antibody, mouse anti-NS5A IgG1, mouse anti-PDI IgG2a, mouse anti-FKBP8 IgG2b, or mouse anti-dsRNA IgG2a (J1 and K2) at 37°C for 60 min; washed three times with PBS containing 1% Tween 20; and incubated with gelatin-PBS containing AF488-conjugated anti-mouse IgG1 or AF647-conjugated anti-rabbit or AF594-conjugated anti-mouse IgG2a or IgG2b antibodies at 37°C for 60 min. Finally, the cells were washed three times with PBS containing 1% Tween 20 and observed with a FluoView FV1000 laser scanning confocal microscope (Olympus, Tokyo, Japan).

Correlative FM-EM. Correlative fluorescence microscopy-electron microscopy (FM-EM) allows individual cells to be examined both in an overview with FM and in a detailed subcellular-structure view with EM (51). The endogenous hB-ind1 and NS5A were stained and observed in the HCV replicon cells by the correlative FM-EM method as described previously (45).

Luciferase assay. Each plasmid was transfected into Huh7, Huh9-13, and interferon (IFN)-cured cells seeded in a 12-well plate, and the cells were treated with 1 μM dexamethasone (Sigma) for 12 h or with 17-dimethylamino-ethylamino-17-demethoxygeldanamycin (DMAG) (Sigma) for 6 h at 36 h posttransfection and lysed in 200 μl of passive lysis buffer (Promega). Luciferase activity was measured in 20-μl aliquots of the cell lysates using a Dual-Luciferase Reporter Assay System (Promega). Firefly luciferase activity was standardized with that of *Renilla* luciferase cotransfected with the internal-control plasmid pRL-TK. The resulting values were expressed as the increase in relative light units (RLU).

Statistical analysis. Results were expressed as the mean ± standard deviation. The significance of differences in the means was determined by Student's *t* test.

RESULTS

The p23-like domain of hB-ind1 has cochaperone activity. Although we had previously reported that hB-ind1 regulates HCV RNA replication through interaction with NS5A and Hsp90, the molecular mechanisms underlying the regulation of HCV replication remained to be clarified. To gain more insights into the potential cochaperone activity of hB-ind1 in the Hsp90 chaperone system, we prepared expression plasmids encoding a wild-type p23 and three p23 mutants—one in which the FXXW motif was replaced with AXXA (p23AxxA), one in which the cochaperone domain of p23 was replaced with the p23-like domain of hB-ind1 (cp23), and one in which both substitutions were made (cp23AxxA) (Fig. 1A). HA-tagged Hsp90 was coexpressed with FLAG-tagged p23 or the FLAG-tagged p23 mutants in 293T cells (Fig. 1B). Hsp90 was coimmunoprecipitated with wild-type p23 and a cp23 mutant, but not with the p23AxxA or cp23AxxA mutants, indicating that the FXXW motif of hB-ind1, as is the case with that of p23

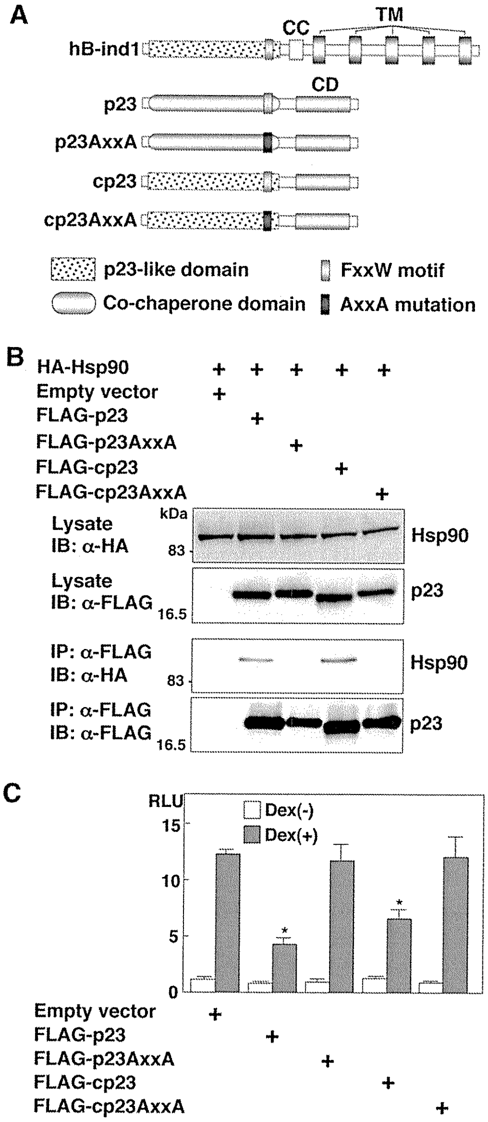

FIG. 1. Construction and characterization of p23 mutants. (A) Structures of hB-ind1, p23, and the three p23 mutants. hB-ind1 consists of a p23-like domain, an FXXW motif, a coiled-coil domain (CC), and a transmembrane domain (TM). p23 consists of a cochaperone domain, an FXXW motif, and a chaperone domain (CD). The three p23 mutants, p23AxxA, cp23, and cp23AxxA, were constructed by replacing the FXXW motif with AXXA, the cochaperone domain of p23 with the p23-like domain of hB-ind1, and both of the regions, respectively. (B) FLAG-tagged p23, p23AxxA, cp23, or cp23AxxA was coexpressed with HA-tagged Hsp90 in 293T cells and immunoprecipitated (IP) with anti-FLAG antibody. The immunoprecipitates were subjected to immunoblotting (IB). (C) The expression plasmid encoding FLAG-tagged p23, cp23, p23AxxA, or cp23AxxA was cotransfected with pGR-luc and pRL-TK plasmids into 293T cells and treated with 1 mM dexamethasone [Dex(+)] at 36 h posttransfection or untreated [Dex(−)], and the luciferase activities were determined at 12 h of incubation. The firefly luciferase activity was normalized with that of *Renilla* luciferase, and the GR-responsive promoter activity was indicated as the RLU. The error bars indicate standard deviations. The asterisks indicate significant differences ($P < 0.01$) versus the control value. The data shown are representative of three independent experiments.

(67), is also involved in binding to Hsp90. Hsp90 participates in the folding and stabilization of the ligand-binding domain of the glucocorticoid receptor (GR), together with p23 and other cofactors (49). p23 was shown to act not only in the activation (30), but also in the inhibition, of GR signaling (67). To examine whether hB-ind1 has the ability to work as a cochaperone in an Hsp90-dependent manner, each of the plasmids encoding p23 or the p23 mutants was cotransfected with a reporter plasmid carrying a firefly luciferase gene under the control of the GR promoter (pGR-luc), together with an internal-control plasmid (pRL-TK), and GR-mediated transcriptional activity was determined at 12 h after treatment with dexamethasone, a ligand of GR. Expression of the p23 or cp23 mutant, but not of the AXXA mutants, significantly inhibited GR-mediated transcription (Fig. 1C). These results indicate that the p23-like domain of hB-ind1 possesses cochaperone activity comparable to that of p23.

The p23-like domain of hB-ind1 is interchangeable with the p23 cochaperone domain during complex formation with NS5A, Hsp90, and FKBP8. Previous reports have suggested that HCV NS5A interacts with several host proteins, including FBL2 (63), vesicle-associated membrane protein-associated protein subtype A (VAP-A) (61), VAP-B (25), FKBP8 (45), and hB-ind1 (56), and that these interactions participate in the replication of HCV. We have shown that hB-ind1 interacts with NS5A and Hsp90 through the coiled-coil domain and the FXXW motif in the p23-like domain, respectively, and that coexpression of FKBP8 enhances the interaction of Hsp90 with hB-ind1 (56). To determine the effect of the mutation in the p23-like domain of hB-ind1 on interaction with Hsp90, NS5A, and FKBP8, we prepared an expression plasmid encoding wild-type hB-ind1 and three hB-ind1 mutants, one in which the p23-like domain was replaced with the cochaperone domain of p23 (chB-ind1), one in which the FXXW motif was replaced with AXXA (hB-ind1AxxA), and one in which both replacements were made (chB-ind1AxxA) (Fig. 2A). The FLAG-tagged wild-type or mutant hB-ind1 was coexpressed with HA-tagged Hsp90 (Fig. 2B, left) or HA-tagged NS5A (Fig. 2B, right) in 293T cells and immunoprecipitated with anti-FLAG antibody. Hsp90 was coprecipitated with wild-type hB-ind1 and the chB-ind1 mutant, but not with the hB-ind1AXXA and chB-ind1AXXA mutants (Fig. 2B, left), confirming that the FXXW motif is crucial for the interaction with Hsp90. In contrast, NS5A was coprecipitated with each of the hB-ind1 proteins, suggesting that mutation in the p23-like domain of hB-ind1 has no effect on the binding of hB-ind1 to NS5A through the coiled-coil domain (Fig. 2B, right). To determine the effect of FKBP8 expression on the interaction between hB-ind1 and Hsp90, FLAG-tagged wild-type hB-ind1 or the chB-ind1 mutant was coexpressed with HA-tagged FKBP8 and/or Hsp90 in 293T cells and immunoprecipitated with anti-FLAG antibody. The amounts of Hsp90 coprecipitated with hB-ind1 or chB-ind1 were increased by coexpression of FKBP8 (Fig. 2C). To further examine the interaction of hB-ind1 with Hsp90 and NS5A at an endogenous expression level in Huh9-13 cells harboring an HCV subgenomic RNA replicon, lysates of the replicon cells were subjected to immunoprecipitation analysis. Endogenous Hsp90 and NS5A were specifically coimmunoprecipitated with endogenous hB-ind1 (Fig. 2D). These results suggest that the p23-like domain of hB-ind1 is interchangeable with the cochaperone domain of p23 during complex formation with NS5A, Hsp90, and FKBP8.

Cochaperone activity in the p23-like domain of hB-ind1 is required for propagation of HCV. The p23-like domain of hB-ind1 has been suggested to be required for HCV propagation (56). However, the involvement of the cochaperone activity of hB-ind1 in HCV propagation has not been examined. To assess the effect of cochaperone activity in the p23-like domain of hB-ind1 on the RNA replication and particle production of HCV, each of the expression plasmids encoding the FLAG-tagged wild-type or mutant hB-ind1 carrying the silent mutations resistant to small interfering RNA was transfected into hB-ind1 knockdown (Huh-KD) cells and cultured for a week in the presence of puromycin. The expressions of FLAG-tagged hB-ind1 and the mutants in the Huh-KD cells were comparable to that of the endogenous hB-ind1 in the control (Huh-ctrl) cells transfected with an empty vector (Fig. 3A). Subgenomic HCV replicon RNA transcribed from pFK-I$_{389}$ neo/NS3-3′/NK5.1 was transfected into these cells and cultured for 4 weeks in the presence of G418. Although the number of colonies was reduced in the Huh-KD cells compared with the Huh-ctrl cells after transfection with an empty vector, as described previously (56), the colony numbers were recovered by the expression of the hB-ind1 or chB-ind1 mutant, but not by that of the hB-ind1AXXA or chB-ind1AXXA mutants (Fig. 3B). Similarly, intracellular HCV RNA and infectious viral titers in the culture supernatants of Huh-KD cells infected with JFH1 virus were partially recovered by the expression of the hB-ind1 or chB-ind1 mutant, but not by that of the hB-ind1AXXA or chB-ind1AXXA mutant (Fig. 3C). These results suggest that cochaperone activity in the p23-like domain of hB-ind1 is required for HCV propagation and that the cochaperone domain of p23 can substitute for the p23-like domain of hB-ind1.

hB-ind1 colocalizes with NS5A, FKBP8, and dsRNA on the membranous web. Our previous report revealed the interplay among hB-ind1, Hsp90, FKBP8, and NS5A and showed that these interactions play an important role in HCV replication (56). However, the subcellular localization of the endogenous hB-ind1 in the replicon cells and JFH1 virus-infected cells has not been precisely assessed. To determine the subcellular localization of hB-ind1 in the context of HCV replication, the expression of hB-ind1 and NS5A in the replicon cells and JFH1 virus-infected cells was examined by immunofluorescence analyses (Fig. 4A). Endogenous hB-ind1 was colocalized with the endoplasmic reticulum (ER)-marker PDI and NS5A as dot-like structures in the Huh9-13 replicon cells (Fig. 4A, top) and in cells infected with JFH1 virus (Fig. 4A, bottom), and these dot-like structures disappeared in concert with the loss of NS5A expression by treatment with IFN-α in the replicon cells and was not observed in the mock-infected Huh7.5.1 cells. Furthermore, FKBP8 (Fig. 4B, top) and dsRNA (Fig. 4B, bottom) were colocalized with hB-ind1 and NS5A in the dot-like structures in Huh9-13 replicon cells. These results indicate that HCV replicating RNA is localized with hB-ind1, FKBP8, and NS5A in the dot-like compartments. HCV RNA replication or expression of viral proteins leads to formation of the convoluted membranous structures designated the membranous web (14, 23). The large structures of the replication complexes in the replicon cells indicate membranous webs with

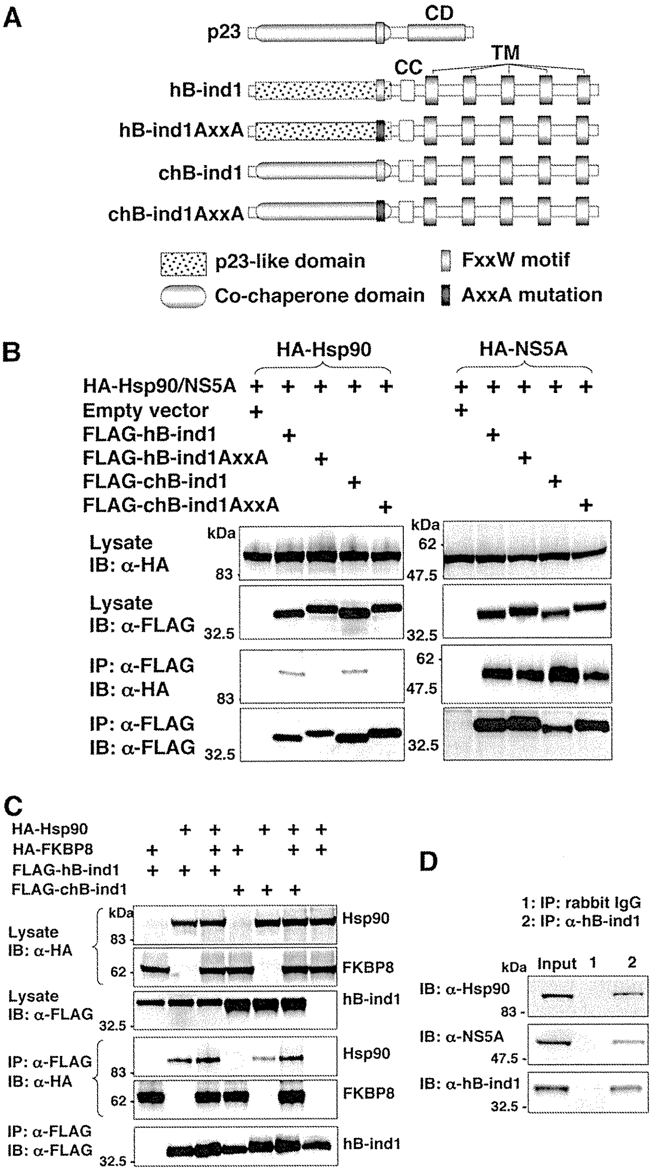

FIG. 2. Construction and characterization of hB-ind1 mutants. (A) Structures of p23, hB-ind1, and the three hB-ind1 mutants. The three hB-ind1 mutants, hB-ind1AxxA, chB-ind1, and chB-ind1AxxA, were constructed by replacing the FXXW motif with AXXA, the p23-like domain of hB-ind1 with the cochaperone domain of p23, and both of the regions, respectively. (B) FLAG-tagged hB-ind1, hB-ind1 AxxA, chB-ind1, or chB-ind1AxxA was coexpressed with either HA-tagged Hsp90 (left) or NS5A (right) in 293T cells and immunoprecipitated (IP) with anti-FLAG antibody. The immunoprecipitates were subjected to immunoblotting (IB). (C) HA-tagged Hsp90 and HA-FKBP8 were expressed with FLAG-tagged hB-ind1 and chB-ind1 in various combinations in 293T cells and immunoprecipitated with anti-FLAG antibody, and the immunoprecipitates were detected by immunoblotting. (D) Endogenous hB-ind1 in Huh9-13 cells harboring subgenomic HCV replicon RNA was immunoprecipitated with anti-hB-ind1 rabbit IgG (lane 2). The cell lysate was mixed with normal rabbit IgG as a negative control (lane 1). The immunoprecipitates were analyzed by immunoblotting with an antibody to Hsp90, NS5A, or hB-ind1. The data shown are representative of three independent experiments.

restricted motility (68). To further analyze the subcellular compartments, including hB-ind1 and NS5A, the same field of the Huh9-13 replicon cells was observed under FM and EM by using the correlative FM-EM technique (Fig. 5A, upper two rows). The large structures that included hB-ind1 and NS5A in the replicon cells were observed under FM and EM (white-boxed areas) and further magnified (black-boxed areas). Convoluted membranous structures that consisted of small vesicles and that were similar to the membranous web were observed. Another field of view yielded similar results (Fig. 5A, lower two rows). The membranous web resembling the convoluted structures was not observed in the Huh9-13 cells depleted of viral RNA by IFN treatment (Fig. 5B). Together, these results suggest that hB-ind1 interacts with NS5A on the membranous web in cells replicating HCV RNA.

Hsp90 is involved in the circumvention of the UPR during HCV replication. Hsp90 regulates the folding and stability of proteins in all eukaryotes (59), and inhibition of the chaperone pathway suppresses correct protein folding, which leads to induction of proteasome-mediated degradation of the unfolded proteins and the unfolded protein response (UPR). Our previous (46) and present studies (Fig. 4 and 5) showed that several cochaperone components are recruited in the membranous web, suggesting that the Hsp90 chaperone system participates in the replication complex to circumvent the induction of the UPR and to maintain the folding of the host and viral proteins in a replication-competent state. To determine the induction of the UPR by HCV replication, Huh9-13 replicon cells were transfected with a reporter plasmid carrying a firefly luciferase gene under the control of the GRP78 promoter, which is activated by the induction of the UPR, together with an internal-control plasmid. Although the GRP78 promoter activity was slightly enhanced in the Huh9-13 cells compared to that in the parental cells, a fourfold increase of GRP78 promoter activity in the replicon cells was observed after treatment with an Hsp90 inhibitor, DMAG, in contrast to the twofold increase in similarly treated parental Huh7 cells, and the activation of the GRP78 promoter was canceled by treatment with IFN-α despite DMAG treatment (Fig. 6A), suggesting that the Hsp90 chaperone system participates in the circumvention of the UPR induced by the replication of HCV RNA. In addition, activation of GRP78 at transcriptional and translational levels after treatment with DMAG was higher in the

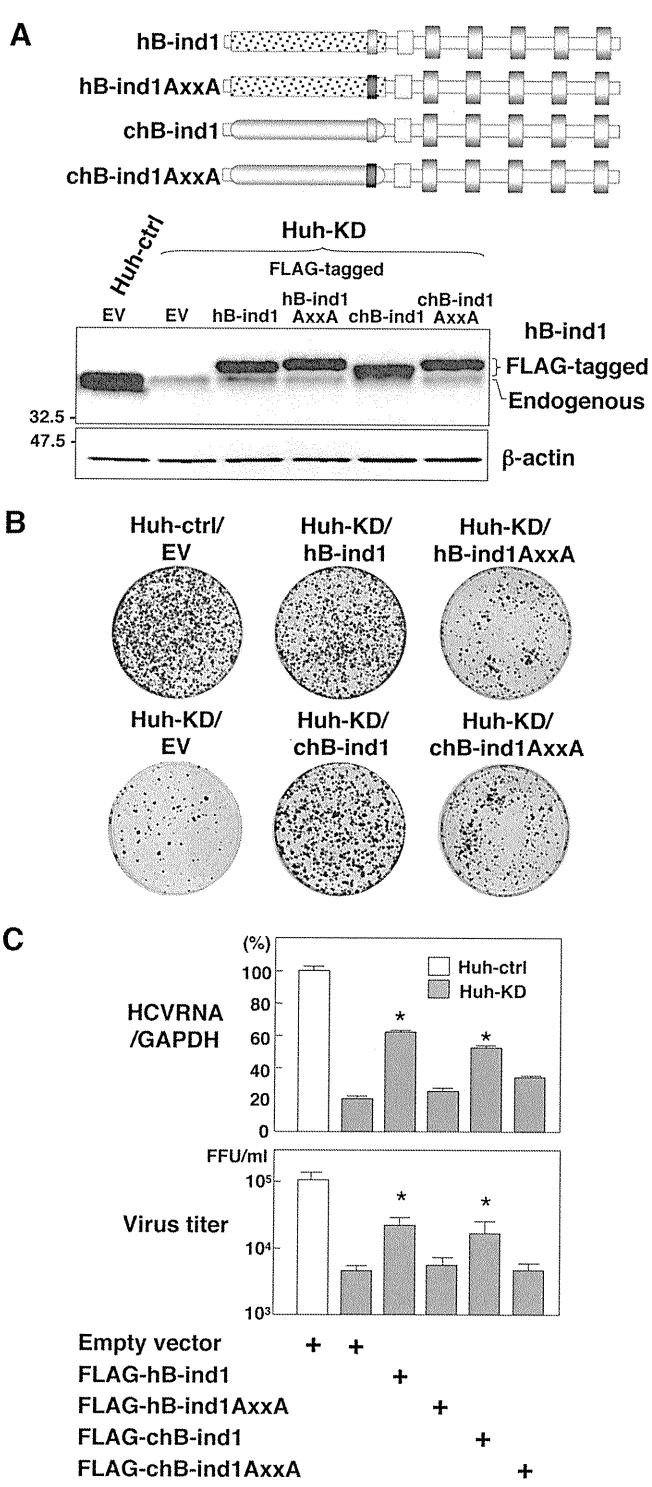

FIG. 3. Effects of the cochaperone activity of hB-ind1 on the propagation of HCV. (A) Huh-KD cells were transfected with either an empty vector or an expression plasmid encoding FLAG-tagged hB-ind1, hB-ind1AxxA, chB-ind1, or chB-ind1AxxA, which are resistant to small interfering RNA due to the introduction of silent mutations, and cultured for a week in the presence of 10 μg/ml of puromycin. The surviving cells were used in the subsequent experiments. The endogenous and exogenous expression of hB-ind1 and the mutants was detected by immunoblotting. The control cell line (Huh-ctrl) or the Huh-KD cell line transfected with an empty vector (EV) was used as a control. (B) Huh-KD cells were transfected with the plasmids and then selected with puromycin. The resulting cells were further transfected with a replicon RNA transcribed from pFK-I_{389} neo/NS3-3′/NK5.1, cultured for 4 weeks in the presence of 1 mg/ml of G418, and stained with crystal violet after fixation with 4% paraformaldehyde. The Huh-KD cell line transfected with an empty vector (EV) was used as a positive control. (C) The cells prepared as described above were infected with JFH1 virus and harvested at 3 days postinfection. The amount of intracellular HCV RNA was estimated by quantitative reverse transcriptase PCR and normalized with that of GAPDH mRNA. The values of HCV RNA are presented as percentages versus those of Huh-ctrl cells transfected with an empty vector. The culture supernatants were subjected to a focus-forming assay. Virus titers are presented as focus-forming units (FFU) per ml. The error bars indicate standard deviations. The asterisks indicate significant differences ($P < 0.01$) versus the value of the control. The data shown are representative of three independent experiments.

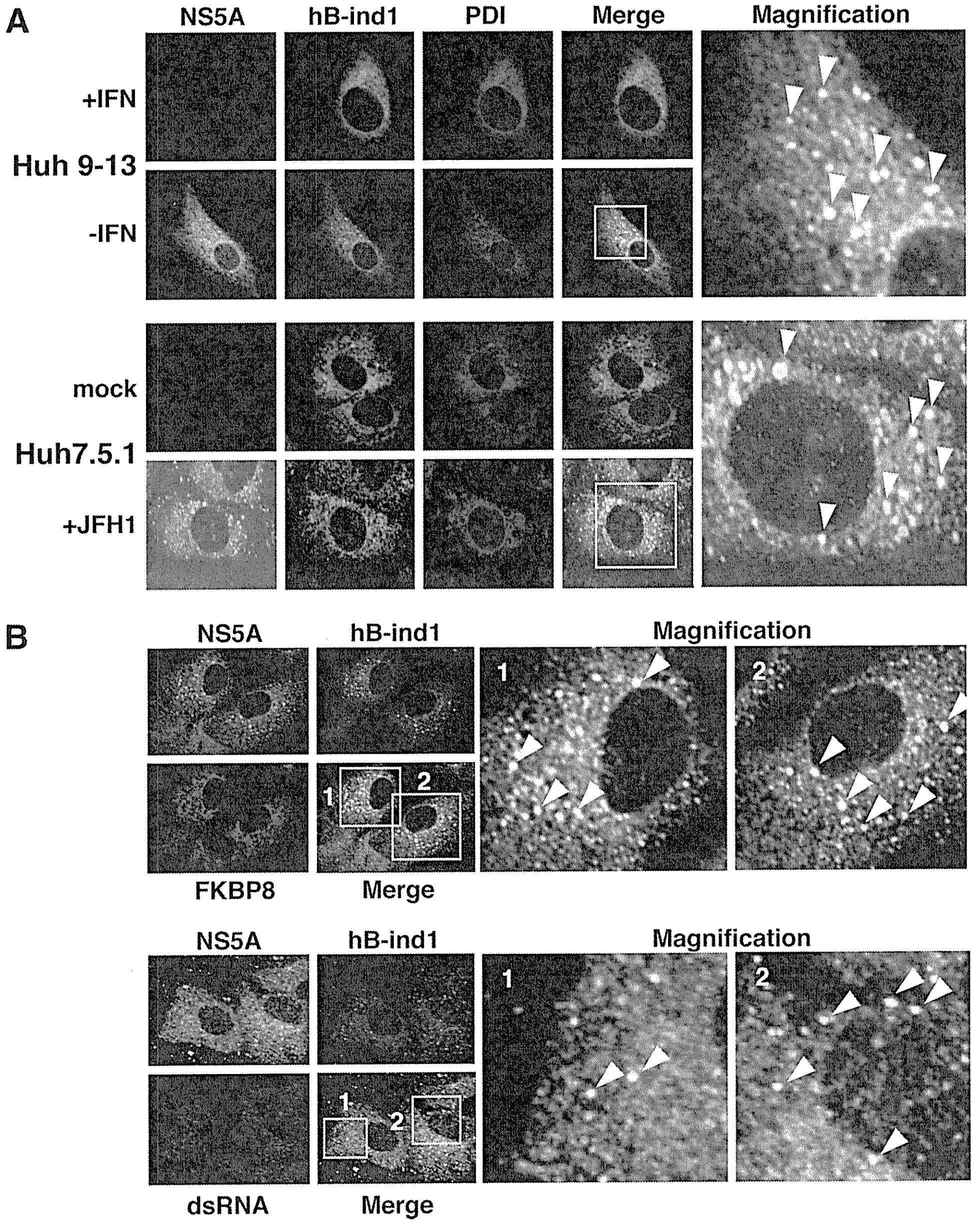

FIG. 4. Intracellular localization of hB-ind1 in replicon cells and infected cells. (A) Huh9-13 replicon cells with IFN-α or untreated and Huh7.5.1 cells infected with JFH1 virus or naïve cells were stained with antibodies against NS5A, hB-ind1, or PDI and examined by immunofluorescence assay. The boxed areas in the merged images are magnified and displayed on the right. The arrowheads indicate intracellular positions colocalized with NS5A, hB-ind1, and PDI. (B) Huh9-13 replicon cells were fixed, permeabilized, and stained with appropriate antibodies to NS5A, hB-ind1, and FKBP8 (top) or dsRNA (bottom). The boxed areas in the merged images are magnified and displayed on the right. The arrowheads indicate intracellular positions colocalized with NS5A, hB-ind, and FKBP8 or dsRNA. The images shown are representative of three independent experiments.

HCV replicon cells than in the parental cells or in cured cells, which were depleted of HCV RNA by treatment with IFN-α (Fig. 6B). Furthermore, DMAG treatment enhanced the transcription of the UPR marker protein GADD153 at a higher level in the replicon cells than in the parental Huh7 or the cured cells (Fig. 6C). These results suggest that the Hsp90-dependent chaperone system plays a crucial role in the folding of the host and viral proteins involved in HCV replication and in the regulation of UPR induction.

DISCUSSION

Studies of the relationship between Hsp90 and steroid receptors, such as GR, have revealed the activities of cochaperones (52, 67). Cochaperones, such as p23, appear to interact with and dissociate from Hsp90 and the client protein complex in a defined order. These cochaperones participate in the chaperone complex in a late step and promote the dissociation of the client proteins from Hsp90 to facilitate formation of the

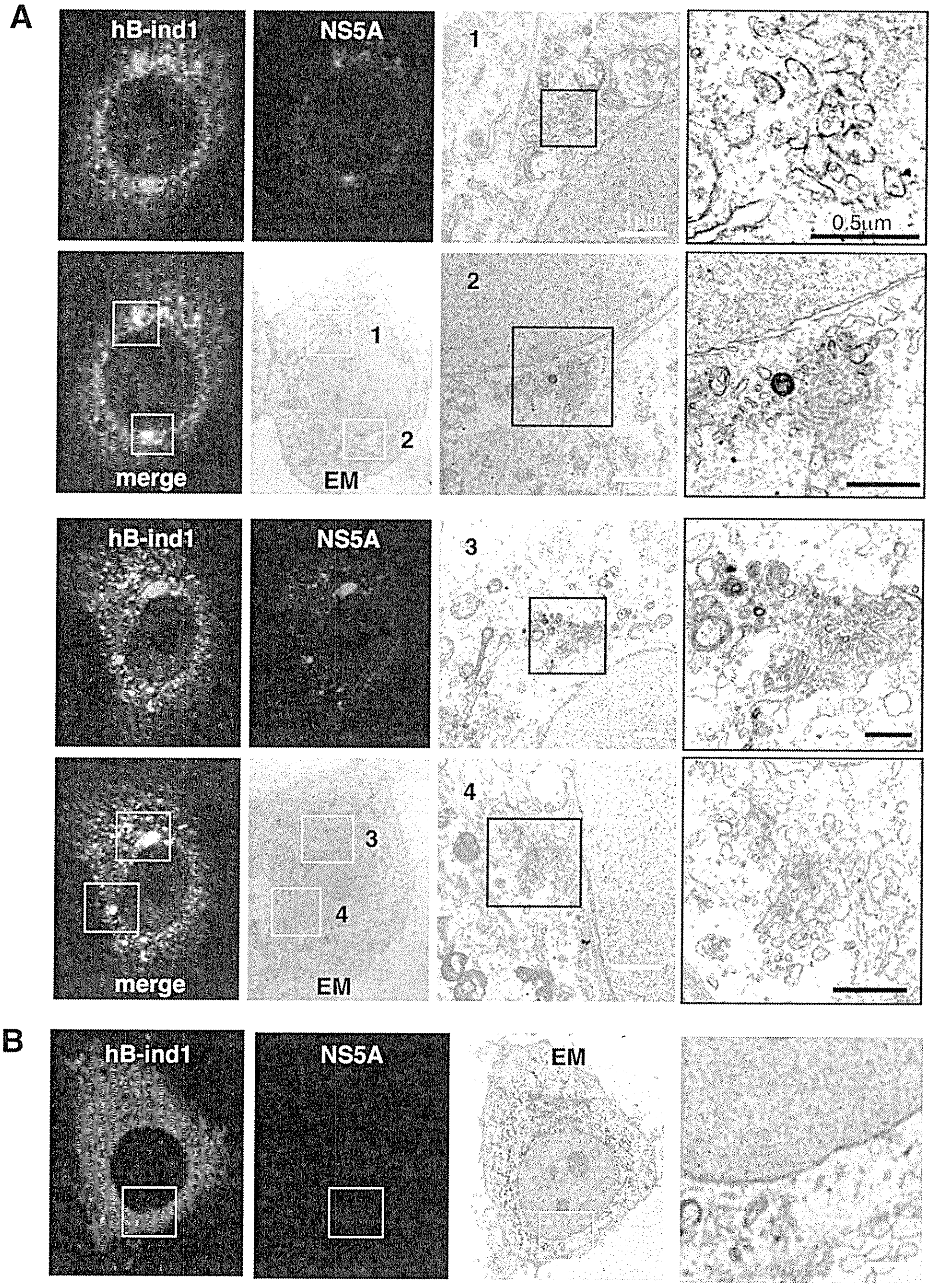

FIG. 5. hB-ind1 interacts with NS5A in the membranous web. Huh9-13 replicon cells were stained with specific antibodies to hB-ind1 and NS5A. Identical fields of Huh9-13 (A) or the cured cells (B) were observed under EM by using the correlative FM-EM technique. The white-boxed areas indicate the colocalized areas of hB-ind1 with NS5A. Magnified views of the white-boxed areas are displayed in the third column from the left. The right column contains further-magnified images of each of the black-boxed areas. Another field of view is presented in the lower two rows.

chaperone complex in the next chaperone cycle (16–18). In this study, we have shown that hB-ind1 participates in HCV replication and that the p23-like domain of hB-ind1 possesses cochaperone activity comparable to that of the cochaperone domain of p23, suggesting that hB-ind1 is involved in the recycling of the chaperone complex in the membranous web to maintain the function of the replication complex of HCV.

Previous studies have indicated that HCV proteins rearrange the ER membrane into the small convoluted membranous vesicles that are collectively known as the membranous web, and these vesicles have been suggested to be the intracellular compartments in which HCV replication takes place (14, 23, 68). In the living replicon cells, two forms of replication complexes, small and large vesicles, are detected, both of which include the viral replication complexes (68). Large vesicles, corresponding to membranous webs, exhibit restricted motil-

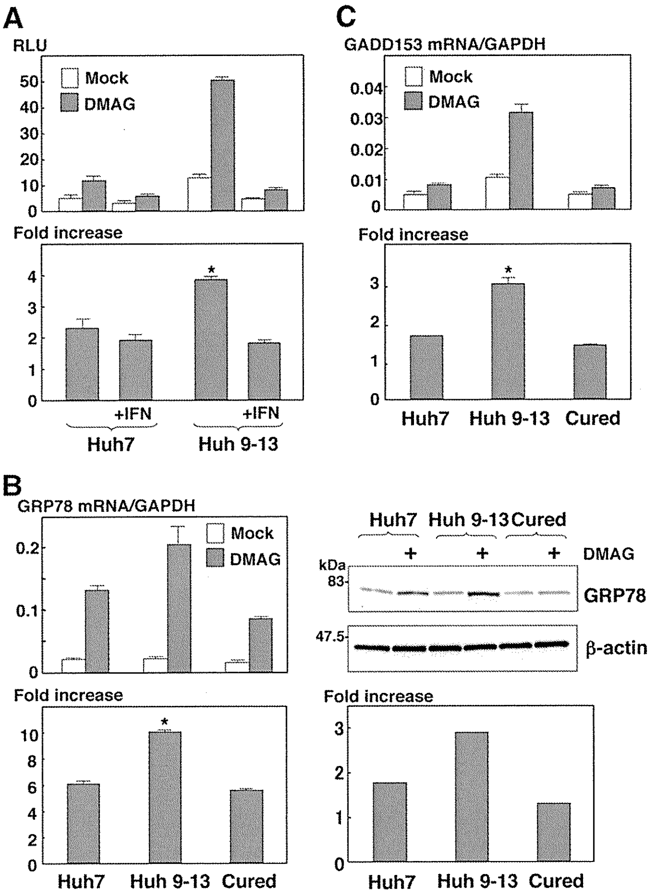

FIG. 6. Effect of Hsp90 inhibitor on the induction of the UPR in HCV replicon cells. (A) Huh7 and Huh9-13 replicon cells were transfected with a reporter plasmid, pGRP78-luc, and an internal-control plasmid, pRL-TK. The transfected cells were treated with IFN-α (+IFN) from 6 to 36 h posttransfection or left untreated and then further incubated for 6 h in the presence or absence of 1 μM DMAG. The resulting cells were harvested and subjected to a dual-luciferase assay. The firefly luciferase activity is indicated as the RLU (top) after standardization with that of *Renilla* luciferase. The enhancement of promoter activity by treatment with DMAG is presented as the increase (bottom). (B) Huh7 cells, Huh9-13 cells, and Huh9-13 cells cured by IFN-α treatment (Cured) were cultured for 6 h in the presence or absence of 1 μM DMAG, and the amount of GRP78 mRNA was measured by real-time PCR. The value of the mRNA was normalized with the amount of GAPDH mRNA (upper left), and the transcriptional enhancement by treatment with DMAG is presented as the increase (lower left). The expression levels of GRP78 and β-actin in the cells were determined by immunoblotting (upper right) and are presented as the increase (lower right). (C) The amounts of GADD153 mRNA in Huh7 cells, Huh9-13 cells, and the cured cells cultured for 6 h in the presence or absence of 1 μM DMAG were measured by real-time PCR. The values of the mRNA were normalized with the amount of GAPDH mRNA (top), and the transcriptional enhancement by treatment with DMAG is presented as the increase (bottom). The error bars indicate standard deviations. The asterisks indicate significant differences ($P < 0.01$) versus the control value. The data shown are representative of three independent experiments.

ity, while small vesicles show fast movement (68), and FM and EM have revealed that NS5A is colocalized with hB-ind1, as well as FKBP8 (45), in the membranous webs. hB-ind1 was first identified as a regulator of Rac1 that activates JNK and NF-κB (11). Rac1 is a member of the Rho GTPase family and plays crucial roles in cytoskeletal dynamics, membrane ruffling, and gene transcription through the effectors of the Rho GTPase family members. IQGAP1 and PAK1 are Rac1 effectors that bind to Rac proteins and are also involved in the replication of HCV (5, 7, 19, 31, 50). The tetratricopeptide repeat domain of immunophilin family members, such as FKBP8, has been shown to interact with Hsp90 (12, 45) and the GR-Hsp90 complex that leads to association with dynein for retrograde transport, along with microtubules (12). Hsp90 has been shown to play an important role in the interaction of transcriptase with genomic RNA of hepatitis B virus (27) and the nuclear transportation of the polymerase of influenza virus (40). Flock house virus also recruits Hsp90 in the polymerase synthesis in the early step of infection (9). Hsp90 may be involved in the regulation of the movement and arrangement of the HCV replication complexes through interaction with Rac1, hB-ind1, and FKBP8. Further investigation is needed to clarify the role of the Hsp90 chaperone system in the life cycle of HCV.

The surrounding membranes, including the membranous web, may protect the viral replication complex and RNA genome against digestion by the host proteases and nucleases (69). The replication complex is composed of viral nonstructural proteins and host proteins, including chaperone and cochaperone proteins. HCV NS5A has been shown to interact with various host proteins, including cochaperones, such as FKBP8 and hB-ind1, and to recruit a chaperone, Hsp90, into the replication complex through interaction with these cochaperones. Recruitment of the chaperone complex into the replication complex is crucial for the correct folding of newly synthesized viral proteins to maintain the efficient replication of the viral genome. HCV replication has been shown to be improved by the adaptive mutations suppressing the phosphorylation status of NS5A in the replicon cells (3). Although suppression of the hyperphosphorylation of NS5A by treatment with kinase inhibitors improves the replication of the replicons that have no adaptive mutations (42), several kinase inhibitors have been shown to suppress the replication of the HCV replicon carrying the adaptive mutations (29), and phosphorylation of NS5A by casein kinase II was shown to improve virus production but not HCV RNA replication (57). Hsp90 is capable of directly modulating the activities of several kinases (37, 53, 54), and thus, it might be feasible that cochaperones, including hB-ind1 and FKBP8, participate in the propagation of HCV by regulating the phosphorylation status of NS5A in cooperation with Hsp90.

The host chaperone system regulates the quality of client proteins, and impairment of the chaperone activity induces accumulation of misfolded proteins and affects the natural cellular function and viability (20, 21, 33). In this study, DMAG treatment induced a higher level of UPR in HCV replicon cells than in parental and cured cells, indicating that the Hsp90 chaperone system participates in the maintenance of correct folding of the viral and host proteins in the replication complex in the membranous web and in the circumvention of the UPR induced by HCV replication. Treatment with geldanamycin or its derivatives has been shown to inhibit GRP94, which is the Hsp90 paralog located in the ER (10), and to disrupt the ER chaperone pathway, leading to the induction of ER-associated protein degradation, transcriptional attenuation, and eventually induction of apoptosis (34). ER chaperones, such as

GRP94, may also participate in the correct folding of the viral and host proteins in the replication complex for efficient replication of the HCV genome.

Geldanamycin and its derivatives have been reported to remarkably inhibit poliovirus replication in vivo without any emergence of drug-resistant escape mutants (22), suggesting that an inhibitor of the chaperone system may be a promising candidate for the treatment of viral infectious diseases with low risk of the emergence of drug-resistant viruses. In addition, Hsp90 inhibitors exhibit anticancer activities through the suppression of various cell signals essential for cancer growth and the enhancement of radiation sensitivity (2, 8, 13). In conclusion, our data indicate that hB-ind1 is included within the HCV replication complex and regulates HCV RNA replication through its own cochaperone activity. Hsp90 and cochaperones, including hB-ind1 and FKBP8, which are required for efficient HCV replication, should be ideal targets for the treatment of chronic hepatitis C with a low frequency of emergence of drug-resistant breakthrough viruses.

ACKNOWLEDGMENTS

We thank H. Murase for her secretarial work. We also thank R. Bartenschlager, T. Wakita, and F. V. Chisari for providing the plasmids and cell lines.

This work was supported in part by grants-in-aid from the Ministry of Health, Labor, and Welfare; the Ministry of Education, Culture, Sports, Science, and Technology; the Global Center of Excellence Program; the Foundation for Biomedical Research and Innovation; and the Naito Foundation.

REFERENCES

1. **Abe, T., Y. Kaname, I. Hamamoto, Y. Tsuda, X. Wen, S. Taguwa, K. Moriishi, O. Takeuchi, T. Kawai, T. Kanto, N. Hayashi, S. Akira, and Y. Matsuura.** 2007. Hepatitis C virus nonstructural protein 5A modulates the toll-like receptor-MyD88-dependent signaling pathway in macrophage cell lines. J. Virol. **81:**8953–8966.
2. **Bisht, K. S., C. M. Bradbury, D. Mattson, A. Kaushal, A. Sowers, S. Markovina, K. L. Ortiz, L. K. Sieck, J. S. Isaacs, M. W. Brechbiel, J. B. Mitchell, L. M. Neckers, and D. Gius.** 2003. Geldanamycin and 17-allylamino-17-demethoxygeldanamycin potentiate the in vitro and in vivo radiation response of cervical tumor cells via the heat shock protein 90-mediated intracellular signaling and cytotoxicity. Cancer Res. **63:**8984–8995.
3. **Blight, K. J., A. A. Kolykhalov, and C. M. Rice.** 2000. Efficient initiation of HCV RNA replication in cell culture. Science **290:**1972–1974.
4. **Bohen, S. P., A. Kralli, and K. R. Yamamoto.** 1995. Hold 'em and fold 'em: chaperones and signal transduction. Science **268:**1303–1304.
5. **Bost, A. G., D. Venable, L. Liu, and B. A. Heinz.** 2003. Cytoskeletal requirements for hepatitis C virus (HCV) RNA synthesis in the HCV replicon cell culture system. J. Virol. **77:**4401–4408.
6. **Brown, G., H. W. Rixon, J. Steel, T. P. McDonald, A. R. Pitt, S. Graham, and R. J. Sugrue.** 2005. Evidence for an association between heat shock protein 70 and the respiratory syncytial virus polymerase complex within lipid-raft membranes during virus infection. Virology **338:**69–80.
7. **Bryan, B. A., D. Li, X. Wu, and M. Liu.** 2005. The Rho family of small GTPases: crucial regulators of skeletal myogenesis. Cell Mol. Life Sci. **62:** 1547–1555.
8. **Calderwood, S. K., M. A. Khaleque, D. B. Sawyer, and D. R. Ciocca.** 2006. Heat shock proteins in cancer: chaperones of tumorigenesis. Trends Biochem. Sci. **31:**164–172.
9. **Castorena, K. M., S. A. Weeks, K. A. Stapleford, A. M. Cadwallader, and D. J. Miller.** 2007. A functional heat shock protein 90 chaperone is essential for efficient flock house virus RNA polymerase synthesis in *Drosophila* cells. J. Virol. **81:**8412–8420.
10. **Chavany, C., E. Mimnaugh, P. Miller, R. Bitton, P. Nguyen, J. Trepel, L. Whitesell, R. Schnur, J. Moyer, and L. Neckers.** 1996. p185erbB2 binds to GRP94 in vivo. Dissociation of the p185erbB2/GRP94 heterocomplex by benzoquinone ansamycins precedes depletion of p185erbB2. J. Biol. Chem. **271:**4974–4977.
11. **Courilleau, D., E. Chastre, M. Sabbah, G. Redeuilh, A. Atfi, and J. Mester.** 2000. B-ind1, a novel mediator of Rac1 signaling cloned from sodium butyrate-treated fibroblasts. J. Biol. Chem. **275:**17344–17348.
12. **Davies, T. H., Y. M. Ning, and E. R. Sanchez.** 2002. A new first step in activation of steroid receptors: hormone-induced switching of FKBP51 and FKBP52 immunophilins. J. Biol. Chem. **277:**4597–4600.
13. **Didelot, C., D. Lanneau, M. Brunet, A. L. Joly, A. De Thonel, G. Chiosis, and C. Garrido.** 2007. Anti-cancer therapeutic approaches based on intracellular and extracellular heat shock proteins. Curr. Med. Chem. **14:**2839–2847.
14. **Egger, D., B. Wolk, R. Gosert, L. Bianchi, H. E. Blum, D. Moradpour, and K. Bienz.** 2002. Expression of hepatitis C virus proteins induces distinct membrane alterations including a candidate viral replication complex. J. Virol. **76:**5974–5984.
15. **Evans, M. J., C. M. Rice, and S. P. Goff.** 2004. Genetic interactions between hepatitis C virus replicons. J. Virol. **78:**12085–12089.
16. **Freeman, B. C., S. J. Felts, D. O. Toft, and K. R. Yamamoto.** 2000. The p23 molecular chaperones act at a late step in intracellular receptor action to differentially affect ligand efficacies. Genes Dev. **14:**422–434.
17. **Freeman, B. C., and K. R. Yamamoto.** 2002. Disassembly of transcriptional regulatory complexes by molecular chaperones. Science **296:**2232–2235.
18. **Frydman, J., and J. Hohfeld.** 1997. Chaperones get in touch: the Hip-Hop connection. Trends Biochem. Sci. **22:**87–92.
19. **Fukata, M., M. Nakagawa, and K. Kaibuchi.** 2003. Roles of Rho-family GTPases in cell polarisation and directional migration. Curr. Opin. Cell Biol. **15:**590–597.
20. **Garrido, C., M. Brunet, C. Didelot, Y. Zermati, E. Schmitt, and G. Kroemer.** 2006. Heat shock proteins 27 and 70: anti-apoptotic proteins with tumorigenic properties. Cell Cycle **5:**2592–2601.
21. **Garrido, C., S. Gurbuxani, L. Ravagnan, and G. Kroemer.** 2001. Heat shock proteins: endogenous modulators of apoptotic cell death. Biochem. Biophys. Res. Commun. **286:**433–442.
22. **Geller, R., M. Vignuzzi, R. Andino, and J. Frydman.** 2007. Evolutionary constraints on chaperone-mediated folding provide an antiviral approach refractory to development of drug resistance. Genes Dev. **21:**195–205.
23. **Gosert, R., D. Egger, V. Lohmann, R. Bartenschlager, H. E. Blum, K. Bienz, and D. Moradpour.** 2003. Identification of the hepatitis C virus RNA replication complex in Huh-7 cells harboring subgenomic replicons. J. Virol. **77:**5487–5492.
24. **Grakoui, A., D. W. McCourt, C. Wychowski, S. M. Feinstone, and C. M. Rice.** 1993. Characterization of the hepatitis C virus-encoded serine proteinase: determination of proteinase-dependent polyprotein cleavage sites. J. Virol. **67:**2832–2843.
25. **Hamamoto, I., Y. Nishimura, T. Okamoto, H. Aizaki, M. Liu, Y. Mori, T. Abe, T. Suzuki, M. M. Lai, T. Miyamura, K. Moriishi, and Y. Matsuura.** 2005. Human VAP-B is involved in hepatitis C virus replication through interaction with NS5A and NS5B. J. Virol. **79:**13473–13482.
26. **Ho, S. N., H. D. Hunt, R. M. Horton, J. K. Pullen, and L. R. Pease.** 1989. Site-directed mutagenesis by overlap extension using the polymerase chain reaction. Gene **77:**51–59.
27. **Hu, J., D. Flores, D. Toft, X. Wang, and D. Nguyen.** 2004. Requirement of heat shock protein 90 for human hepatitis B virus reverse transcriptase function. J. Virol. **78:**13122–13131.
28. **Huang, D. C., S. Cory, and A. Strasser.** 1997. Bcl-2, Bcl-XL and adenovirus protein E1B19kD are functionally equivalent in their ability to inhibit cell death. Oncogene **14:**405–414.
29. **Huang, Y., K. Staschke, R. De Francesco, and S. L. Tan.** 2007. Phosphorylation of hepatitis C virus NS5A nonstructural protein: a new paradigm for phosphorylation-dependent viral RNA replication? Virology **364:**1–9.
30. **Hutchison, K. A., L. F. Stancato, J. K. Owens-Grillo, J. L. Johnson, P. Krishna, D. O. Toft, and W. B. Pratt.** 1995. The 23-kDa acidic protein in reticulocyte lysate is the weakly bound component of the hsp foldosome that is required for assembly of the glucocorticoid receptor into a functional heterocomplex with hsp90. J. Biol. Chem. **270:**18841–18847.
31. **Ishida, H., K. Li, M. Yi, and S. M. Lemon.** 2007. p21-activated kinase 1 is activated through the mammalian target of rapamycin/p70 S6 kinase pathway and regulates the replication of hepatitis C virus in human hepatoma cells. J. Biol. Chem. **282:**11836–11848.
32. **Kampmueller, K. M., and D. J. Miller.** 2005. The cellular chaperone heat shock protein 90 facilitates Flock House virus RNA replication in *Drosophila* cells. J. Virol. **79:**6827–6837.
33. **Kim, H. P., D. Morse, and A. M. Choi.** 2006. Heat-shock proteins: new keys to the development of cytoprotective therapies. Exp. Opin. Ther. Targets **10:**759–769.
34. **Lai, E., T. Teodoro, and A. Volchuk.** 2007. Endoplasmic reticulum stress: signaling the unfolded protein response. Physiology **22:**193–201.
35. **Lohmann, V., F. Korner, J. Koch, U. Herian, L. Theilmann, and R. Bartenschlager.** 1999. Replication of subgenomic hepatitis C virus RNAs in a hepatoma cell line. Science **285:**110–113.
36. **McLauchlan, J., M. K. Lemberg, G. Hope, and B. Martoglio.** 2002. Intramembrane proteolysis promotes trafficking of hepatitis C virus core protein to lipid droplets. EMBO J. **21:**3980–3988.
37. **Miyata, Y., and I. Yahara.** 1992. The 90-kDa heat shock protein, HSP90, binds and protects casein kinase II from self-aggregation and enhances its kinase activity. J. Biol. Chem. **267:**7042–7047.
38. **Momose, F., T. Naito, K. Yano, S. Sugimoto, Y. Morikawa, and K. Nagata.**

2002. Identification of Hsp90 as a stimulatory host factor involved in influenza virus RNA synthesis. J. Biol. Chem. **277:**45306–45314.

39. **Moradpour, D., F. Penin, and C. M. Rice.** 2007. Replication of hepatitis C virus. Nat. Rev. Microbiol. **5:**453–463.
40. **Naito, T., F. Momose, A. Kawaguchi, and K. Nagata.** 2007. Involvement of Hsp90 in assembly and nuclear import of influenza virus RNA polymerase subunits. J. Virol. **81:**1339–1349.
41. **Neckers, L.** 2002. Hsp90 inhibitors as novel cancer chemotherapeutic agents. Trends Mol. Med. **8:**S55–S61.
42. **Neddermann, P., M. Quintavalle, C. Di Pietro, A. Clementi, M. Cerretani, S. Altamura, L. Bartholomew, and R. De Francesco.** 2004. Reduction of hepatitis C virus NS5A hyperphosphorylation by selective inhibition of cellular kinases activates viral RNA replication in cell culture. J. Virol. **78:**13306–13314.
43. **Okamoto, K., Y. Mori, Y. Komoda, T. Okamoto, M. Okochi, M. Takeda, T. Suzuki, K. Moriishi, and Y. Matsuura.** 2008. Intramembrane processing by signal peptide peptidase regulates the membrane localization of hepatitis C virus core protein and viral propagation. J. Virol. **82:**8349–8361.
44. **Okamoto, K., K. Moriishi, T. Miyamura, and Y. Matsuura.** 2004. Intramembrane proteolysis and endoplasmic reticulum retention of hepatitis C virus core protein. J. Virol. **78:**6370–6380.
45. **Okamoto, T., Y. Nishimura, T. Ichimura, K. Suzuki, T. Miyamura, T. Suzuki, K. Moriishi, and Y. Matsuura.** 2006. Hepatitis C virus RNA replication is regulated by FKBP8 and Hsp90. EMBO J. **25:**5015–5025.
46. **Okamoto, T., H. Omori, Y. Kaname, T. Abe, Y. Nishimura, T. Suzuki, T. Miyamura, T. Yoshimori, K. Moriishi, and Y. Matsuura.** 2008. A single-amino-acid mutation in hepatitis C virus NS5A disrupting FKBP8 interaction impairs viral replication. J. Virol. **82:**3480–3489.
47. **Pietschmann, T., V. Lohmann, A. Kaul, N. Krieger, G. Rinck, G. Rutter, D. Strand, and R. Bartenschlager.** 2002. Persistent and transient replication of full-length hepatitis C virus genomes in cell culture. J. Virol. **76:**4008–4021.
48. **Prapapanich, V., S. Chen, E. J. Toran, R. A. Rimerman, and D. F. Smith.** 1996. Mutational analysis of the hsp70-interacting protein Hip. Mol. Cell. Biol. **16:**6200–6207.
49. **Pratt, W. B., and D. O. Toft.** 1997. Steroid receptor interactions with heat shock protein and immunophilin chaperones. Endocr. Rev. **18:**306–360.
50. **Ridley, A. J., H. F. Paterson, C. L. Johnston, D. Diekmann, and A. Hall.** 1992. The small GTP-binding protein rac regulates growth factor-induced membrane ruffling. Cell **70:**401–410.
51. **Rieder, C. L., and S. S. Bowser.** 1985. Correlative immunofluorescence and electron microscopy on the same section of epon-embedded material. J. Histochem. Cytochem. **33:**165–171.
52. **Sanchez, E. R., D. O. Toft, M. J. Schlesinger, and W. B. Pratt.** 1985. Evidence that the 90-kDa phosphoprotein associated with the untransformed L-cell glucocorticoid receptor is a murine heat shock protein. J. Biol. Chem. **260:**12398–12401.
53. **Sato, S., N. Fujita, and T. Tsuruo.** 2000. Modulation of Akt kinase activity by binding to Hsp90. Proc. Natl. Acad. Sci. USA **97:**10832–10837.
54. **Stancato, L. F., A. M. Silverstein, J. K. Owens-Grillo, Y. H. Chow, R. Jove, and W. B. Pratt.** 1997. The hsp90-binding antibiotic geldanamycin decreases Raf levels and epidermal growth factor signaling without disrupting formation of signaling complexes or reducing the specific enzymatic activity of Raf kinase. J. Biol. Chem. **272:**4013–4020.
55. **Stravopodis, D. J., L. H. Margaritis, and G. E. Voutsinas.** 2007. Drug-mediated targeted disruption of multiple protein activities through functional inhibition of the Hsp90 chaperone complex. Curr. Med. Chem. **14:**3122–3138.
56. **Taguwa, S., T. Okamoto, T. Abe, Y. Mori, T. Suzuki, K. Moriishi, and Y. Matsuura.** 2008. Human butyrate-induced transcript 1 interacts with hepatitis C virus NS5A and regulates viral replication. J. Virol. **82:**2631–2641.
57. **Tellinghuisen, T. L., K. L. Foss, and J. Treadaway.** 2008. Regulation of hepatitis C virion production via phosphorylation of the NS5A protein. PLoS Pathog. **4:**e1000032.
58. **Tellinghuisen, T. L., J. Marcotrigiano, and C. M. Rice.** 2005. Structure of the zinc-binding domain of an essential component of the hepatitis C virus replicase. Nature **435:**374–379.
59. **Terasawa, K., M. Minami, and Y. Minami.** 2005. Constantly updated knowledge of Hsp90. J. Biochem. **137:**443–447.
60. **Tomei, L., C. Failla, E. Santolini, R. De Francesco, and N. La Monica.** 1993. NS3 is a serine protease required for processing of hepatitis C virus polyprotein. J. Virol. **67:**4017–4026.
61. **Tu, H., L. Gao, S. T. Shi, D. R. Taylor, T. Yang, A. K. Mircheff, Y. Wen, A. E. Gorbalenya, S. B. Hwang, and M. M. Lai.** 1999. Hepatitis C virus RNA polymerase and NS5A complex with a SNARE-like protein. Virology **263:**30–41.
62. **Wakita, T., T. Pietschmann, T. Kato, T. Date, M. Miyamoto, Z. Zhao, K. Murthy, A. Habermann, H. G. Krausslich, M. Mizokami, R. Bartenschlager, and T. J. Liang.** 2005. Production of infectious hepatitis C virus in tissue culture from a cloned viral genome. Nat. Med. **11:**791–796.
63. **Wang, C., M. Gale, Jr., B. C. Keller, H. Huang, M. S. Brown, J. L. Goldstein, and J. Ye.** 2005. Identification of FBL2 as a geranylgeranylated cellular protein required for hepatitis C virus RNA replication. Mol. Cell **18:**425–434.
64. **Wasley, A., and M. J. Alter.** 2000. Epidemiology of hepatitis C: geographic differences and temporal trends. Semin. Liver Dis. **20:**1–16.
65. **Watashi, K., N. Ishii, M. Hijikata, D. Inoue, T. Murata, Y. Miyanari, and K. Shimotohno.** 2005. Cyclophilin B is a functional regulator of hepatitis C virus RNA polymerase. Mol. Cell **19:**111–122.
66. **Whitesell, L., and S. L. Lindquist.** 2005. HSP90 and the chaperoning of cancer. Nat. Rev. Cancer. **5:**761–772.
67. **Wochnik, G. M., J. C. Young, U. Schmidt, F. Holsboer, F. U. Hartl, and T. Rein.** 2004. Inhibition of GR-mediated transcription by p23 requires interaction with Hsp90. FEBS Lett. **560:**35–38.
68. **Wolk, B., B. Buchele, D. Moradpour, and C. M. Rice.** 2008. A dynamic view of hepatitis C virus replication complexes. J. Virol. **82:**10519–10531.
69. **Yang, G., D. C. Pevear, M. S. Collett, S. Chunduru, D. C. Young, C. Benetatos, and R. Jordan.** 2004. Newly synthesized hepatitis C virus replicon RNA is protected from nuclease activity by a protease-sensitive factor(s). J. Virol. **78:**10202–10205.
70. **Zhong, J., P. Gastaminza, G. Cheng, S. Kapadia, T. Kato, D. R. Burton, S. F. Wieland, S. L. Uprichard, T. Wakita, and F. V. Chisari.** 2005. Robust hepatitis C virus infection in vitro. Proc. Natl. Acad. Sci. USA **102:**9294–9299.

JOURNAL OF VIROLOGY, Mar. 2009, p. 2389–2392
0022-538X/09/$08.00+0 doi:10.1128/JVI.01690-08
Vol. 83, No. 5

Proteasomal Turnover of Hepatitis C Virus Core Protein Is Regulated by Two Distinct Mechanisms: a Ubiquitin-Dependent Mechanism and a Ubiquitin-Independent but PA28γ-Dependent Mechanism▽

Ryosuke Suzuki,[1] Kohji Moriishi,[2] Kouichirou Fukuda,[1] Masayuki Shirakura,[1] Koji Ishii,[1] Ikuo Shoji,[3] Takaji Wakita,[1] Tatsuo Miyamura,[1] Yoshiharu Matsuura,[2] and Tetsuro Suzuki[1]*

Department of Virology II, National Institute of Infectious Diseases, Tokyo 162-8640,[1] Department of Molecular Virology, Research Institute for Microbial Diseases, Osaka University, Osaka 565-0871,[2] and Division of Microbiology, Kobe University Graduate School of Medicine, Hyogo 650-0017,[3] Japan

Received 8 August 2008/Accepted 5 December 2008

We have previously reported on the ubiquitylation and degradation of hepatitis C virus core protein. Here we demonstrate that proteasomal degradation of the core protein is mediated by two distinct mechanisms. One leads to polyubiquitylation, in which lysine residues in the N-terminal region are preferential ubiquitylation sites. The other is independent of the presence of ubiquitin. Gain- and loss-of-function analyses using lysineless mutants substantiate the hypothesis that the proteasome activator PA28γ, a binding partner of the core, is involved in the ubiquitin-independent degradation of the core protein. Our results suggest that turnover of this multifunctional viral protein can be tightly controlled via dual ubiquitin-dependent and -independent proteasomal pathways.

Hepatitis C virus (HCV) core protein, whose amino acid sequence is highly conserved among different HCV strains, not only is involved in the formation of the HCV virion but also has a number of regulatory functions, including modulation of signaling pathways, cellular and viral gene expression, cell transformation, apoptosis, and lipid metabolism (reviewed in references 9 and 15). We have previously reported that the E6AP E3 ubiquitin (Ub) ligase binds to the core protein and plays an important role in polyubiquitylation and proteasomal degradation of the core protein (22). Another study from our group identified the proteasome activator PA28γ/REG-γ as an HCV core-binding partner, demonstrating degradation of the core protein via a PA28γ-dependent pathway (16, 17). In this work, we further investigated the molecular mechanisms underlying proteasomal degradation of the core protein and found that in addition to regulation by the Ub-mediated pathway, the turnover of the core protein is also regulated by PA28γ in a Ub-independent manner.

Although ubiquitylation of substrates generally requires at least one Lys residue to serve as a Ub acceptor site (5), there is no consensus as to the specificity of the Lys targeted by Ub (4, 8). To determine the sites of Ub conjugation in the core protein, we used site-directed mutagenesis to replace individual Lys residues or clusters of Lys residues with Arg residues in the N-terminal 152 amino acids (aa) of the core (C152), within which is contained all seven Lys residues (Fig. 1A). Plasmids expressing a variety of mutated core proteins were generated by PCR and inserted into the pCAGGS (18). Each core-expressing construct was transfected into human embryonic kidney 293T cells along with the pMT107 (25) encoding a Ub moiety tagged with six His residues (His_6). Transfected cells were treated with the proteasome inhibitor MG132 for 14 h to maximize the level of Ub-conjugated core intermediates by blocking the proteasome pathway and were harvested 48 h posttransfection. His_6-tagged proteins were purified from the extracts by Ni^{2+}-chelation chromatography. Eluted protein and whole lysates of transfected cells before purification were analyzed by Western blotting using anticore antibodies (Fig. 1B). Mutations replacing one or two Lys residues with Arg in the core protein did not affect the efficiency of ubiquitylation: detection of multiple Ub-conjugated core intermediates was observed in the mutant core proteins comparable to the results seen with the wild-type core protein as previously reported (23). In contrast, a substitution of four N-terminal Lys residues (C152K6-23R) caused a significant reduction in ubiquitylation (Fig. 1B, lane 9). Multiple Ub-conjugated core intermediates were not detected in the Lys-less mutant (C152KR), in which all seven Lys residues were replaced with Arg (Fig. 1B, lane 11). These results suggest that there is not a particular Lys residue in the core protein to act as the Ub acceptor but that more than one Lys located in its N-terminal region can serve as the preferential ubiquitylation site. In rare cases, Ub is known to be conjugated to the N terminus of proteins; however, these results indicate that this does not occur within the core protein.

To investigate how polyubiquitylation correlates with proteasome degradation of the core protein, we performed kinetic analysis of the wild-type and mutated core proteins by use of the Ub protein reference (UPR) technique, which can compensate for data scatter of sample-to-sample variations such as levels of expression (10, 24). Fusion proteins expressed from UPR-based constructs (Fig. 2A) were cotranslationally cleaved by deubiquitylating enzymes, thereby generating equimolar quantities of the core proteins and the reference protein, dihydrofolate reductase-hemagglutinin (DHFR-HA) tag-modified Ub, in which the Lys at aa 48 was replaced by Arg to prevent its polyubiquitylation (Ub^{R48}). After 24 h of transfec-

---

* Corresponding author. Mailing address: Department of Virology II, National Institute of Infectious Diseases, 1-23-1 Toyama, Shinjuku-ku, Tokyo 162-8640, Japan. Phone: 81-3-5285-1111. Fax: 81-3-5285-1161. E-mail: tesuzuki@nih.go.jp.

▽ Published ahead of print on 17 December 2008.

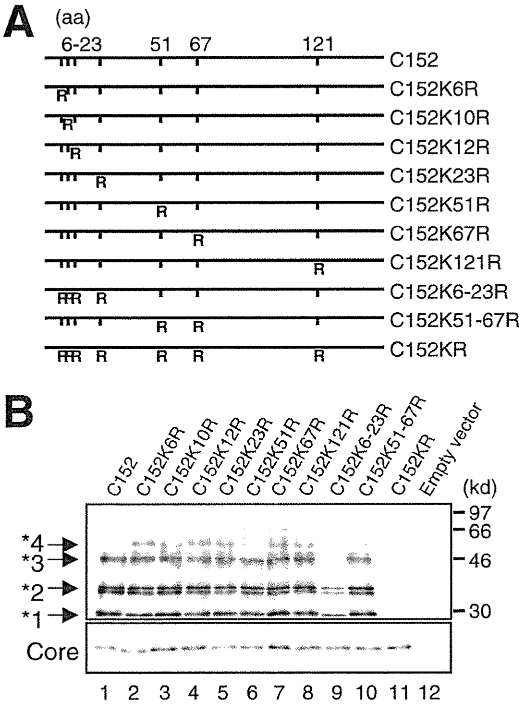

FIG. 1. In vivo ubiquitylation of HCV core protein. (A) The HCV core protein (N-terminal 152 aa) is represented on the top. The positions of the amino acid residues of the core protein are indicated above the bold lines. The positions of the seven Lys residues in the core are marked by vertical ticks. Substitution of Lys with Arg (R) is schematically depicted. (B) Detection of ubiquitylated forms of the core proteins. The transfected cells with core expression plasmids and pMT107 were treated with the proteasome inhibitor MG132 and harvested 48 h after transfection. His$_6$-tagged proteins were purified and subsequently analyzed by Western blot analysis using anticore antibody (upper panel). Core proteins conjugated to a number of His$_6$-Ub are denoted with asterisks. Whole lysates of transfected cells before purification were also analyzed (lower panel). Lanes 1 to 11, C152 to C152KR, as indicated for panel A. Lane 12; empty vector.

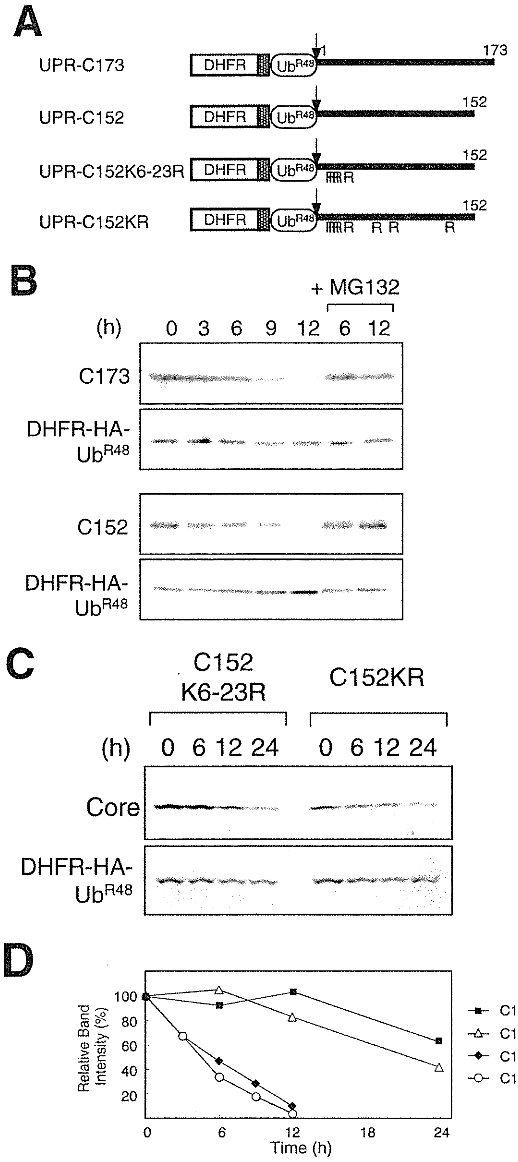

FIG. 2. Kinetic analysis of degradation of HCV core proteins. (A) The fusion constructs used in the UPR technique. Open boxes indicate the DHFR sequence, which is extended at the C terminus by a sequence containing the HA epitope (hatched boxes). Ub^{R48} moieties bearing the Lys-Arg substitution at aa 48 are represented by open ellipses. Bold lines indicate the regions of the core protein. The amino acid positions of the core protein are indicated above the bold lines. The arrows indicate the sites of in vivo cleavage by deubiquitylating enzymes. (B and C) Turnover of the core proteins. After a 24-h transfection with each UPR construct, cells were treated with 50 μg of cycloheximide/ml in the presence or absence of 10 μM MG132 for the different time periods indicated. Cells were lysed at the different time points indicated, followed by evaluation via sodium dodecyl sulfate-polyacrylamide gel electrophoresis and Western blot analysis using antibodies against the core protein and HA. (D) Quantitation of the data shown in panels B and C. At each time point, the ratio of band intensity of the core protein relative to the reference DHFR-HA-Ub^{R48} was determined by densitometry and is plotted as a percentage of the ratio at time zero.

tion with UPR constructs, cells were treated with cycloheximide and the amounts of core proteins and DHFR-HA-Ub^{R48} at the indicated time points were determined by Western blot analysis using anticore and anti-HA antibodies. The mature form of the core protein, aa 1 to 173 (C173) (13, 20), and C152 were degraded with first-order kinetics (Fig. 2B and D). MG132 completely blocked the degradation of C173 and C152 (Fig. 2B), and C152K6-23R and C152KR were markedly stabilized (Fig. 2C). The half-lives of C173 and C152 were calculated to be 5 to 6 h, whereas those of C152K6-23R and C152KR were calculated to be 22 to 24 h (Fig. 2D), confirming that the Ub plays an important role in regulating degradation of the core protein. Nevertheless, these results also suggest possible involvement of the Ub-independent pathway in the turnover of the core protein, as C152KR is more destabilized than the reference protein (Fig. 2C and 2D).

We have shown that PA28γ specifically binds to the core protein and is involved in its degradation (16, 17). Recent studies demonstrated that PA28γ is responsible for Ub-independent degradation of the steroid receptor coactivator SRC-3 and cell cycle inhibitors such as p21 (3, 11, 12). Thus, we next investigated the possibility of PA28γ involvement in the degradation of either C152KR or C152. Since C152KR carries two amino acid substitutions in the PA28γ-binding region (aa 44 to 71) (17), we tested the influence of the mutations of C152KR on the interaction with PA28γ by use of a coimmunoprecipitation assay. When Flag-tagged PA28γ (F-PA28γ) was expressed in cells along with C152 or C152KR, F-PA28γ precipitated along with both C152 and C152KR, indicating that PA28γ interacts with both core proteins (Fig. 3A). Figure 3B reveals the effect of exogenous expression of F-PA28γ on the steady-state levels of C152 and C152KR. Consistent with previous data (17), the expression level of C152 was decreased to a nearly undetectable level in the presence of PA28γ (Fig. 3B, lanes 1 and 3). Interestingly, exogenous expression of PA28γ led to a marked reduction in the amount of C152KR expressed (Fig. 3B, lanes 5 and 7). Treatment with MG132 increased the steady-state level of the C152KR in the presence of F-PA28γ as well as the level of C152 (Fig. 3B, lanes 4 and 8).

We further investigated whether PA28γ affects the turnover of Lys-less core protein through time course experiments. C152KR was rapidly destabilized and almost completely degraded in a 3-h chase experiment using cells overexpressing F-PA28γ (Fig. 3C, left panels). A similar result was obtained using an analogous Lys-less mutant of the full-length core protein C191KR (Fig. 3C, right panels), thus demonstrating that the Lys-less core protein undergoes proteasomal degradation in a PA28γ-dependent manner. These results suggest that PA28γ may play a role in accelerating the turnover of the HCV core protein that is independent of ubiquitylation.

Finally, we examined gain- and loss-of-function of PA28γ with respect to degradation of full-length wild-type (C191) and mutated (C191KR) core proteins in human hepatoma Huh-7 cells. As expected, exogenous expression of PA28γ or E6AP caused a decrease in the C191 steady-state levels (Fig. 4A). In contrast, the C191KR level was decreased with expression of PA28γ but not of E6AP. We further used RNA interference to inhibit expression of PA28γ or E6AP. An increase in the abundance of C191KR was observed with PA28γ small interfering RNA (siRNA) but not with E6AP siRNA (Fig. 4B). An increase in the C191 level caused by the activity of siRNA against PA28γ or E6AP was confirmed as well.

Taking these results together, we conclude that turnover of the core protein is regulated by both Ub-dependent and Ub-independent pathways and that PA28γ is possibly involved in Ub-independent proteasomal degradation of the core protein. PA28 is known to specifically bind and activate the 20S proteasome (19). Thus, PA28γ may function by facilitating the delivery of the core protein to the proteasome in a Ub-independent manner.

Accumulating evidence suggests the existence of proteasome-dependent but Ub-independent pathways for protein degradation, and several important molecules, such as p53, p73, Rb, SRC-3, and the hepatitis B virus X protein, have two distinct degradation pathways that function in a Ub-dependent and Ub-independent manner (1, 2, 6, 7, 14, 21, 27). Recently, critical roles for PA28γ in the Ub-independent pathway have been demonstrated; SRC-3 and p21 can be recognized by the 20S proteasome independently of ubiquitylation through their interaction with PA28γ (3, 11, 12). It has also been reported that phosphorylation-dependent ubiquitylation mediated by GSK3 and SCF is important for SRC-3 turnover (26). Nevertheless, the precise mechanisms underlying turnover of most of the proteasome substrates that are regulated in both Ub-dependent and Ub-independent manners are not well understood. To our knowledge, the HCV core protein is the first

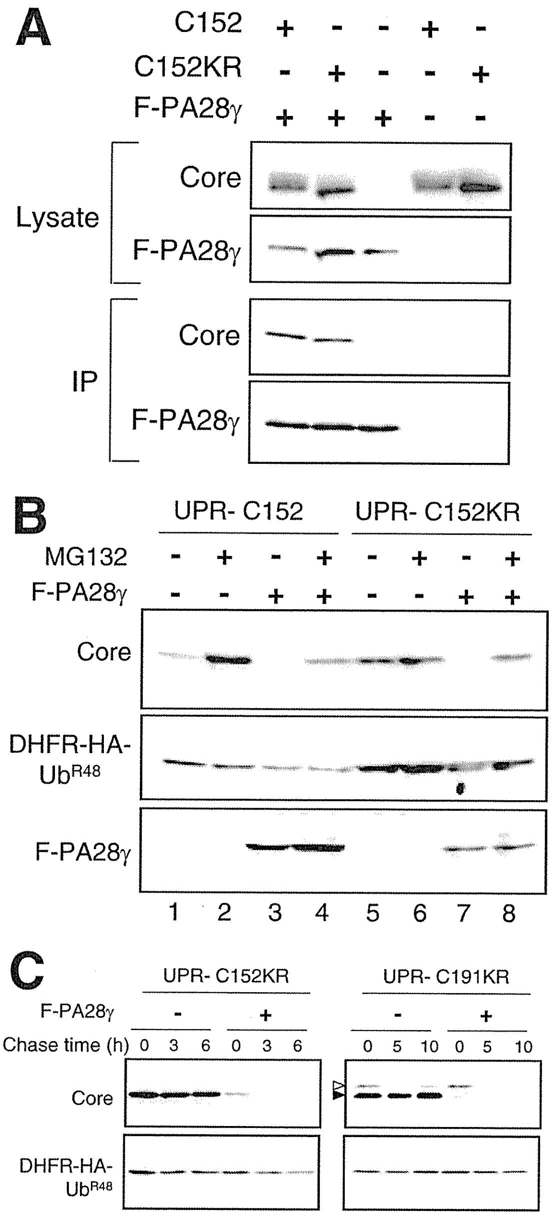

FIG. 3. PA28γ-dependent degradation of the core protein. (A) Interaction of the core protein with PA28γ. Cells were cotransfected with the wild-type (C152) or Lys-less (C152KR) core expression plasmid in the presence of a Flag-PA28γ (F-PA28γ) expression plasmid or an empty vector. The transfected cells were treated with MG132. After 48 h, the cell lysates were immunoprecipitated with anti-Flag antibody and visualized by Western blotting with anticore antibodies. Western blot analysis of whole cell lysates was also performed. (B) Degradation of the wild-type and Lys-less core proteins via the PA28γ-dependent pathway. Cells were transfected with the UPR construct with or without F-PA28γ. In some cases, cells were treated with 10 μM MG132 for 14 h before harvesting. Western blot analysis was performed using anticore, anti-HA, and anti-Flag antibodies. (C) After 24 h of transfection with UPR-C152KR and UPR-C191KR with or without F-PA28γ (an empty vector), cells were treated with 50 μg of cycloheximide/ml for different time periods as indicated (chase time). Western blot analysis was performed using anticore and anti-HA antibodies. The precursor core protein and the core that was processed, presumably by signal peptide peptidase, are denoted by open and closed triangles, respectively.

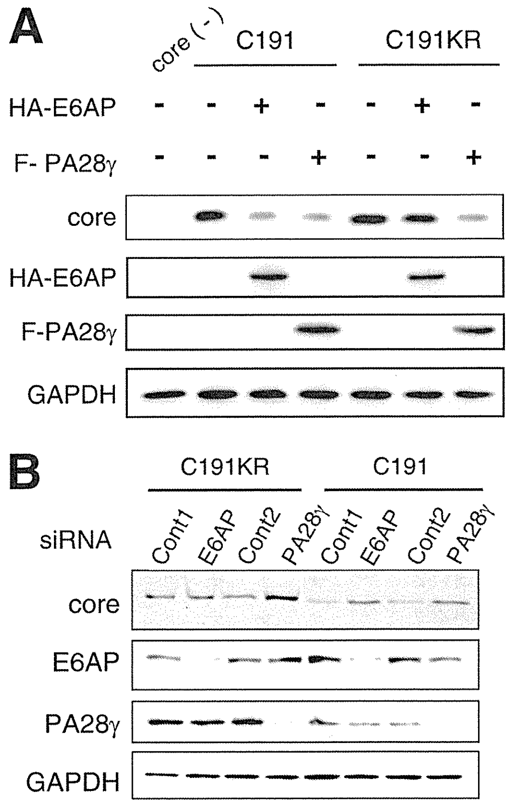

FIG. 4. Ub-dependent and Ub-independent degradation of the full-length core protein in hepatic cells. (A) Huh-7 cells were cotransfected with plasmids for the full-length core protein (C191) or its Lys-less mutant (C191KR) in the presence of F-PA28γ or HA-tagged-E6AP expression plasmid (HA-E6AP). After 48 h, cells were lysed and Western blot analysis was performed using anticore, anti-HA, anti-Flag, or anti-GAPDH. (B) Huh-7 cells were cotransfected with core expression plasmids along with siRNA against PA28γ or E6AP or with negative control siRNA. Cells were harvested 72 h after transfection and subjected to Western blot analysis.

viral protein studied that has led to identification of key cellular factors responsible for proteasomal degradation via dual distinct mechanisms. Although the question remains whether there is a physiological significance of the Ub-dependent and Ub-independent degradation of the core protein, it is reasonable to consider that tight control over cellular levels of the core protein, which is multifunctional and essential for viral replication, maturation, and pathogenesis, may play an important role in representing the potential for its functional activity.

This work was supported by a grant-in-aid for Scientific Research from the Japan Society for the Promotion of Science, from the Ministry of Health, Labor and Welfare of Japan, and from the Ministry of Education, Culture, Sports, Science and Technology, by Research on Health Sciences focusing on Drug Innovation from the Japan Health Sciences Foundation, Japan, and by the Program for Promotion of Fundamental Studies in Health Sciences of the National Institute of Biomedical Innovation of Japan.

REFERENCES

1. **Asher, G., J. Lotem, L. Sachs, C. Kahana, and Y. Shaul.** 2002. Mdm-2 and ubiquitin-independent p53 proteasomal degradation regulated by NQO1. Proc. Natl. Acad. Sci. USA **99:**13125–13130.
2. **Asher, G., P. Tsvetkov, C. Kahana, and Y. Shaul.** 2005. A mechanism of ubiquitin-independent proteasomal degradation of the tumor suppressors p53 and p73. Genes Dev. **19:**316–321.
3. **Chen, X., L. F. Barton, Y. Chi, B. E. Clurman, and J. M. Roberts.** 2007. Ubiquitin-independent degradation of cell-cycle inhibitors by the REGγ proteasome. Mol. Cell **26:**843–852.
4. **Ciechanover, A.** 1998. The ubiquitin-proteasome pathway: on protein death and cell life. EMBO J. **17:**7151–7160.
5. **Hershko, A., A. Ciechanover, and A. Varshavsky.** 2000. The ubiquitin system. Nat. Med. **6:**1073–1081.
6. **Jariel-Encontre, I., M. Pariat, F. Martin, S. Carillo, C. Salvat, and M. Piechaczyk.** 1995. Ubiquitinylation is not an absolute requirement for degradation of c-Jun protein by the 26 S proteasome. J. Biol. Chem. **270:**11623–11627.
7. **Jin, Y., H. Lee, S. X. Zeng, M. S. Dai, and H. Lu.** 2003. MDM2 promotes p21waf1/cip1 proteasomal turnover independently of ubiquitylation. EMBO J. **22:**6365–6377.
8. **Ju, D., and Y. Xie.** 2006. Identification of the preferential ubiquitination site and ubiquitin-dependent degradation signal of Rpn4. J. Biol. Chem. **281:**10657–10662.
9. **Lai, M. M. C., and C. F. Ware.** 1999. Hepatitis C virus core protein: possible roles in viral pathogenesis. Springer, Berlin, Germany.
10. **Lévy, F., N. Johnsson, T. Rumenapf, and A. Varshavsky.** 1996. Using ubiquitin to follow the metabolic fate of a protein. Proc. Natl. Acad. Sci. USA **93:**4907–4912.
11. **Li, X., L. Amazit, W. Long, D. M. Lonard, J. J. Monaco, and B. W. O'Malley.** 2007. Ubiquitin- and ATP-independent proteolytic turnover of p21 by the REGγ-proteasome pathway. Mol. Cell **26:**831–842.
12. **Li, X., D. M. Lonard, S. Y. Jung, A. Malovannaya, Q. Feng, J. Qin, S. Y. Tsai, M. J. Tsai, and B. W. O'Malley.** 2006. The SRC-3/AIB1 coactivator is degraded in a ubiquitin- and ATP-independent manner by the REGγ proteasome. Cell **124:**381–392.
13. **Liu, Q., C. Tackney, R. A. Bhat, A. M. Prince, and P. Zhang.** 1997. Regulated processing of hepatitis C virus core protein is linked to subcellular localization. J. Virol. **71:**657–662.
14. **Lonard, D. M., Z. Nawaz, C. L. Smith, and B. W. O'Malley.** 2000. The 26S proteasome is required for estrogen receptor-α and coactivator turnover and for efficient estrogen receptor-α transactivation. Mol. Cell **5:**939–948.
15. **Moradpour, D., F. Penin, and C. M. Rice.** 2007. Replication of hepatitis C virus. Nat. Rev. Microbiol. **5:**453–463.
16. **Moriishi, K., R. Mochizuki, K. Moriya, H. Miyamoto, Y. Mori, T. Abe, S. Murata, K. Tanaka, T. Miyamura, T. Suzuki, K. Koike, and Y. Matsuura.** 2007. Critical role of PA28γ in hepatitis C virus-associated steatogenesis and hepatocarcinogenesis. Proc. Natl. Acad. Sci. USA **104:**1661–1666.
17. **Moriishi, K., T. Okabayashi, K. Nakai, K. Moriya, K. Koike, S. Murata, T. Chiba, K. Tanaka, R. Suzuki, T. Suzuki, T. Miyamura, and Y. Matsuura.** 2003. Proteasome activator PA28γ-dependent nuclear retention and degradation of hepatitis C virus core protein. J. Virol. **77:**10237–10249.
18. **Niwa, H., K. Yamamura, and J. Miyazaki.** 1991. Efficient selection for high-expression transfectants with a novel eukaryotic vector. Gene **108:**193–199.
19. **Realini, C., C. C. Jensen, Z. Zhang, S. C. Johnston, J. R. Knowlton, C. P. Hill, and M. Rechsteiner.** 1997. Characterization of recombinant REGα, REGβ, and REGγ proteasome activators. J. Biol. Chem. **272:**25483–25492.
20. **Santolini, E., G. Migliaccio, and N. La Monica.** 1994. Biosynthesis and biochemical properties of the hepatitis C virus core protein. J. Virol. **68:**3631–3641.
21. **Sheaff, R. J., J. D. Singer, J. Swanger, M. Smitherman, J. M. Roberts, and B. E. Clurman.** 2000. Proteasomal turnover of p21Cip1 does not require p21Cip1 ubiquitination. Mol. Cell **5:**403–410.
22. **Shirakura, M., K. Murakami, T. Ichimura, R. Suzuki, T. Shimoji, K. Fukuda, K. Abe, S. Sato, M. Fukasawa, Y. Yamakawa, M. Nishijima, K. Moriishi, Y. Matsuura, T. Wakita, T. Suzuki, P. M. Howley, T. Miyamura, and I. Shoji.** 2007. E6AP ubiquitin ligase mediates ubiquitylation and degradation of hepatitis C virus core protein. J. Virol. **81:**1174–1185.
23. **Suzuki, R., K. Tamura, J. Li, K. Ishii, Y. Matsuura, T. Miyamura, and T. Suzuki.** 2001. Ubiquitin-mediated degradation of hepatitis C virus core protein is regulated by processing at its carboxyl terminus. Virology **280:**301–309.
24. **Suzuki, T., and A. Varshavsky.** 1999. Degradation signals in the lysine-asparagine sequence space. EMBO J. **18:**6017–6026.
25. **Treier, M., L. M. Staszewski, and D. Bohmann.** 1994. Ubiquitin-dependent c-Jun degradation in vivo is mediated by the δ domain. Cell **78:**787–798.
26. **Wu, R. C., Q. Feng, D. M. Lonard, and B. W. O'Malley.** 2007. SRC-3 coactivator functional lifetime is regulated by a phospho-dependent ubiquitin time clock. Cell **129:**1125–1140.
27. **Zhang, Z., and R. Zhang.** 2008. Proteasome activator PA28γ regulates p53 by enhancing its MDM2-mediated degradation. EMBO J. **27:**852–864.

JOURNAL OF VIROLOGY, Aug. 2009, p. 7959–7969
0022-538X/09/$08.00+0 doi:10.1128/JVI.00889-09
Vol. 83, No. 16

Human VAP-C Negatively Regulates Hepatitis C Virus Propagation[▽]

Hiroshi Kukihara,[1] Kohji Moriishi,[1] Shuhei Taguwa,[1] Hideki Tani,[1] Takayuki Abe,[1]
Yoshio Mori,[1] Tetsuro Suzuki,[2] Takasuke Fukuhara,[1,3] Akinobu Taketomi,[3]
Yoshihiko Maehara,[3] and Yoshiharu Matsuura[1]*

Department of Molecular Virology, Research Institute for Microbial Diseases, Osaka University, Osaka,[1] Department of Virology II, National Institute of Infectious Diseases, Tokyo,[2] and Department of Surgery and Science, Graduate School of Medical Sciences, Kyushu University, Fukuoka,[3] Japan

Received 3 May 2009/Accepted 2 June 2009

Human vesicle-associated membrane protein-associated protein (VAP) subtype A (VAP-A) and subtype B (VAP-B) are involved in the regulation of membrane trafficking, lipid transport and metabolism, and the unfolded protein response. VAP-A and VAP-B consist of the major sperm protein (MSP) domain, the coiled-coil motif, and the C-terminal transmembrane anchor and form homo- and heterodimers through the transmembrane domain. VAP-A and VAP-B interact with NS5B and NS5A of hepatitis C virus (HCV) through the MSP domain and the coiled-coil motif, respectively, and participate in the replication of HCV. VAP-C is a splicing variant of VAP-B consisting of the N-terminal half of the MSP domain of VAP-B followed by the subtype-specific frameshift sequences, and its biological function has not been well characterized. In this study, we have examined the biological functions of VAP-C in the propagation of HCV. VAP-C interacted with NS5B but not with VAP-A, VAP-B, or NS5A in immunoprecipitation analyses, and the expression of VAP-C inhibited the interaction of NS5B with VAP-A or VAP-B. Overexpression of VAP-C impaired the RNA replication of the HCV replicon and the propagation of the HCV JFH1 strain, whereas overexpression of VAP-A and VAP-B enhanced the replication. Furthermore, the expression of VAP-C was observed in various tissues, whereas it was barely detected in the liver. These results suggest that VAP-C acts as a negative regulator of HCV propagation and that the expression of VAP-C may participate in the determination of tissue tropism of HCV propagation.

Hepatitis C virus (HCV) is a major causative agent of chronic liver disease and thus a major public health problem, infecting at least 3% of the world population (47). HCV infection proceeds to the persistent stage in approximately 80% of patients, leading to the development of cirrhosis in 20% to 50% of patients, of whom approximately 5% eventually develop hepatocellular carcinoma (12). HCV encompasses a single-stranded positive-sense RNA genome of approximately 9.6 kb, which encodes a large precursor polyprotein comprising approximately 3,000 amino acids (26). The structural proteins are cleaved from the N-terminal one-fourth of the polyprotein by the host signal peptidase and signal peptide peptidase (23, 32, 33), resulting in the maturation of the capsid protein, two envelope proteins and viroporin p7. The NS2 protease cleaves after the carboxyl terminus, and then NS3 cleaves the appropriate downstream positions to produce NS4A, NS4B, NS5A, and NS5B (8, 42), all of which form the replication complex along with several host proteins (5, 21). NS5B is the RNA-dependent RNA polymerase, which is a main enzymatic component of the replication complex of HCV (3), while NS5A is a membrane-anchored zinc-binding phosphoprotein that appears to possess diverse functions, including the suppression of host defense and the regulation of the virus's replication (1, 4, 6, 41), although its biological function remains unclear.

The NS5A protein has been shown to interact with several host proteins, including vesicle-associated membrane protein (VAMP)-associated protein (VAP) subtype A (VAP-A) (44) and subtype B (VAP-B) (9), FKBP8 (34), MyD88 (1), FBL2 (46), human butyrate-induced transcript 1 (hB-ind1) (40), and so on (25). VAP-A and VAP-B also bind to NS5B, although it remains unclear whether these interactions modulate HCV replication positively or negatively (9, 44). VAP-A and VAP-B have been shown to associate with the cytoplasmic face of the endoplasmic reticulum (ER) and the Golgi apparatus (38) and to consist of the major sperm protein (MSP) domain, the coiled-coil domain, and the transmembrane (TM) region, in that order (30, 39), as shown in Fig. 1A. VAP was originally reported as a protein binding to VAMP, which is a synaptic vesicle SNARE protein required for synaptic-vesicle fusion in the nematode *Aplysia californica*, and was designated the 33-kDa VAMP-associated protein, VAP-33 (39). Two mammalian homologues, VAP-A and VAP-B, were subsequently identified (30, 38). The transcription of VAP-A and VAP-B is ubiquitously detected in mammalian organs, including the heart, placenta, lung, liver, skeletal muscle, and pancreas (30), suggesting that VAP family proteins are involved in diverse cellular functions other than neurotransmitter release (30, 38, 49). Several VAP-interacting proteins share the FFAT motif (two phenylalanines in an acidic tract), which has the consensus amino acid sequence EFFDAXE, as determined by a comparison among oxysterol binding proteins (OSBPs), OSBP-related proteins (ORPs) (20), and the ceramide transport protein CERT (10, 19), contributing to the regulation of fatty acid metabolism. The interaction of VAP family proteins with

---

* Corresponding author. Mailing address: Department of Molecular Virology, Research Institute for Microbial Diseases, Osaka University, 3-1, Yamadaoka, Suita, Osaka 565-0871, Japan. Phone: 81-6-6879-8340. Fax: 81-6-6879-8269. E-mail: matsuura@biken.osaka-u.ac.jp.

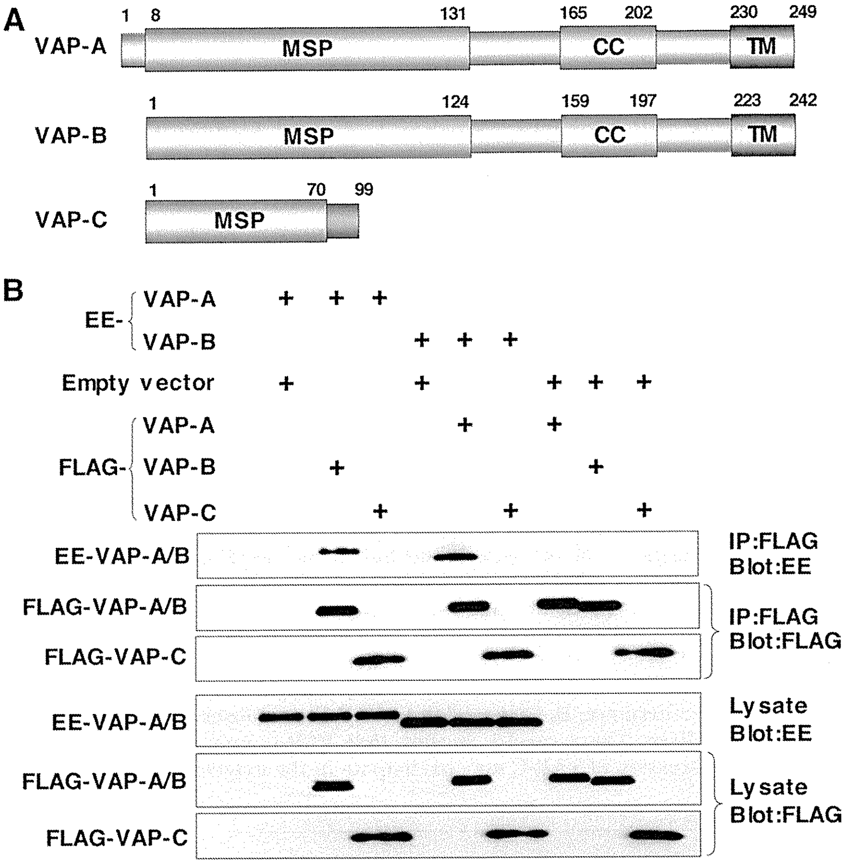

FIG. 1. VAP-C interacts with neither VAP-A nor VAP-B. (A) Structures of VAP family proteins. The MSP domain, the coiled-coil domain, and the TM region are indicated as MSP, CC, and TM, respectively. (B) Interaction among VAP family proteins. The expression plasmids encoding VAP proteins or empty vector (1 μg each) were transfected into 293T cells, FLAG-tagged VAP proteins coexpressed with EE-tagged VAP-A or VAP-B were immunoprecipitated (IP) with anti-FLAG antibody, and the resulting precipitates were examined by immunoblotting using anti-FLAG or anti-EE antibody. One percent of the volume of the lysate was used as an input control. The data in each panel are representative of the results of three independent experiments. +, present.

other host proteins, including VAMP and tubulin, is independent of the FFAT motif (16, 36, 38, 50). The third subtype of VAP is VAP-C, which is an alternative spliced isoform of VAP-B, consisting of the N-terminal half of the MSP domain and the subtype-specific 29 amino acids (Fig. 1A). However, its tissue distribution and physiological function remain largely unknown.

Glutathione *S*-transferase pulldown and immunoprecipitation analyses revealed that both VAP-A and VAP-B interact with NS5B and NS5A through the MSP domain and the coiled-coil domain, respectively (9, 44), and the MSP domains of VAP-A and VAP-B exhibit 82.3% homology. Although VAP-C possesses the N-terminal-half region of the MSP domain of VAP-B, the biological significance of VAP-C in the propagation of HCV has not yet been clarified. In this study, we examined the expression of VAP-C in human tissues and the effects of VAP-C expression on the RNA replication, translation, and particle formation of HCV.

MATERIALS AND METHODS

Cell lines. Cells of the human hepatoma cell line Huh-7, cell line Huh7OK1, and embryonic kidney cell line 293T were maintained in Dulbecco's modified Eagle's medium (DMEM) (Sigma, St. Louis, MO) containing 10% fetal calf serum (FCS) and nonessential amino acids (NEAA), while Huh 9-13 cells, which possess a subgenomic HCV RNA replicon of genotype 1b (21), were cultured in DMEM supplemented with 10% FCS, NEAA, and 1 mg/ml G418. The Huh7OK1 cell line exhibits the highest efficiency of propagation of strain JFH1 virus, as described previously (35). All cell lines were cultured at 37°C in a humidified atmosphere with 5% CO_2.

Antibodies. Chicken anti-human VAP-B antibody was described previously (9). Rabbit anti-human VAP-C antibody was prepared by immunization using synthetic peptides of the amino acid residues from 86 to 98, QPHFSISPNW EGR, which region does not share the homology to VAP-A and VAP-B. The mouse monoclonal antibody to human VAP-A was purchased from BD Pharmingen (San Diego, CA). Mouse monoclonal antibodies to influenza virus hemagglutinin (HA) and the GluGlu (EE) tag were from Covance (Richmond, CA). Mouse and rabbit anti-FLAG antibodies and mouse anti-β-actin monoclonal antibody were from Sigma. Rabbit polyclonal antibody to NS5A was prepared as described previously (34). Mouse anti-NS5A monoclonal antibody was from Austral Biologicals (San Ramon, CA).

Plasmids. A cDNA clone encoding NS5A was amplified from HCV genotype 1b strain J1 (9) (GenBank database accession number D89815) by PCR, using *Pfu* turbo DNA polymerase (Stratagene, La Jolla, CA). The fragments were then cloned into the appropriate sites in pEF-FLAG pGBK puro (13). The DNA fragment encoding NS5B of the J1 strain was generated by PCR and cloned into pCAGGs-PUR (31). The DNA fragment encoding human VAP-A was amplified by PCR from a human fetal-brain library (Clontech, Palo Alto, CA) and was introduced into pEF-FLAG pGBK puro and pEF-EE hygro (13), as described previously (9). A DNA fragment encoding VAP-C was amplified from cDNA of hepatoma cell line Huh-7 and was introduced into pEF-FLAG pGBK puro. Pro^{56}-to-Ser (P56S) mutants of VAPs were generated by site-directed mutagenesis (11). All PCR products were confirmed by sequencing with an ABI Prism 3130 genetic analyzer (Applied Biosystems, Tokyo, Japan).

Transfection, immunoblotting, and immunoprecipitation. Cells were seeded onto a six-well tissue culture plate 24 h before transfection. The plasmids were transfected into cells by liposome-mediated transfection using TransIT LT1 (Mirus Bio, Madison, WI). These transfected cells were harvested at 36 h posttransfection, washed three times with 1 ml of ice-cold phosphate-buffered saline (PBS), and suspended in 0.2 ml lysis buffer (20 mM Tris-HCl, pH 7.4, containing 135 mM NaCl and 1% Triton X-100) supplemented with protease inhibitor cocktail (Roche, Indianapolis, IN). The cell lysates were sonicated at 4°C for 5 min, incubated for 30 min at 4°C, and centrifuged at 15,000 rpm for 30 min at 4°C. The supernatant was subjected to immunoprecipitation analyses as described previously (27). The immunoprecipitated proteins were boiled in 30 μl of loading buffer and then subjected to sodium dodecyl sulfate–12.5% polyacrylamide gel electrophoresis. The proteins were transferred to polyvinylidene difluoride membranes (Millipore, Bedford, MA) and then reacted with primary antibody and secondary horseradish peroxidase-conjugated antibody. The immunocomplexes were visualized with Super Signal West Femto substrate (Pierce, Rockford, IL) and detected by using an LAS-3000 image analyzer (Fujifilm, Tokyo, Japan). The distribution of VAPs in human organs was determined by using premade human tissue lysates (Protein medleys; Clonetech), which are aliquots of various organ lysates prepared from samples from several people, and liver tissues obtained during surgery after approval of the ethical committee of Kyushu University Graduate School of Medicine.

Real-time PCR. The HCV genomic RNA was determined by the method described previously (40). Total RNA was prepared from cells by using an RNeasy mini kit (Qiagen, Tokyo, Japan). First-strand cDNA was synthesized using an RNA LA PCR kit (Takara Bio, Inc., Shiga, Japan) and random primers. Expression of the appropriate gene was estimated by using platinum SYBR green quantitative PCR SuperMix UDG (Invitrogen, Carlsbad, CA) according to the manufacturer's protocol. Fluorescent signals were estimated by using an ABI Prism 7000 system (Applied Biosystems). The 5′ untranslated region of HCV and the glyceraldehyde-3-phosphate dehydrogenase (GAPDH) mRNA were amplified using primer pairs described previously (40). The amount of HCV genomic RNA was normalized with that of GAPDH mRNA.

Focus-forming assay. The viral RNA of the JFH1 strain was introduced into the Huh7OK1 cell line according to the method of Zhong et al. (51). The culture supernatant was collected at 7 days posttransfection and used as the infectious HCV particles. Huh7OK1 cells in DMEM containing 10% FCS were seeded at 5×10^4 cells per well into a 24-well plate 12 h before infection. The cells were infected with the JFH1 strain at a multiplicity of infection (MOI) of 0.05 and incubated at 37°C for 2 h. The medium was replaced with fresh DMEM containing 10% FCS and NEAA at 2 h postinfection. The cells were fixed with 4% paraformaldehyde at 96 h postinfection and permeabilized with PBS containing 0.2% Triton X-100. These fixed and permeabilized cells were stained with the anti-NS5A mouse monoclonal antibody and Alexa Fluor (AF) 488-conjugated antibody to mouse immunoglobulin G (Molecular Probes, Eugene, OR). Clusters of infected cells stained with the NS5A antibody were derived from a single infectious focus, and virus titers were represented as focus-forming units/ml.

Quantification of the HCV core protein by ELISA. The HCV core protein was quantified by using an Ortho HCV antigen enzyme-linked immunosorbent assay (ELISA) test (Ortho Clinical Diagnostics, Tokyo, Japan) according to the manufacturer's instructions. To determine the intracellular expression of core protein, Huh7OK1 cells were infected with the infectious HCV particles described above, lysed with the lysis buffer on ice, and applied to the ELISA after 100- to 10,000-fold dilution with PBS. Total protein was quantified by using a Micro BCA protein assay reagent kit (Pierce). The intracellular and extracellular levels of expression of the core protein were normalized by the total amount of protein.

Effect of the VAP expression on the cap-independent translational activity of the viral IRES. The cDNA fragment encoding a firefly luciferase was excised from a pGL3 basic plasmid (Promega, Madison, WI) and introduced into the downstream region of the *Renilla* luciferase gene of pRL-CMV (cytomegalovirus) (Promega). Then, the cDNA fragments encoding the internal ribosome entry site (IRES) of the HCV strains Con1 and JFH1 were introduced between the *Renilla* and firefly luciferase genes, and the resulting plasmids were designated pRL-CMV-HCVCon1 and pRL-CMV-HCVJFH1, respectively (see Fig. 4A). The IRES region of HCV was replaced with that of poliovirus (PV) or encephalomyocarditis virus (EMCV), and the plasmids designated pRL-CMV-PV and pRL-CMV-EMCV, respectively (see Fig. 4B). Each reporter plasmid was introduced into Huh7OK1 cells that had been transfected with the expression plasmid encoding FLAG-green fluorescent protein (GFP), FLAG–VAP-A, FLAG–VAP-B, or FLAG–VAP-C 24 h previously, and cells were harvested at 48 h posttransfection. Luciferase activities in cells were measured by using a dual-luciferase reporter assay system (Promega). The activity of firefly luciferase was normalized with that of *Renilla* luciferase and represented as relative luciferase activity (RLU).

Indirect immunofluorescence assay. The Huh 9-13 cells were cultured on glass slides and transfected with the expression plasmids encoding FLAG-tagged VAPs, P56S VAP mutants, or empty vector. The resulting cells were fixed at 72 h posttransfection with 4% paraformaldehyde in PBS at room temperature for 30 min. After being washed twice with PBS, cells were permeabilized for 20 min at room temperature with PBS containing 0.25% saponin and blocked with PBS containing 1% bovine serum albumin (BSA-PBS) for 60 min at room temperature. The cells were then incubated with BSA-PBS containing rabbit anti-FLAG and mouse anti-NS5A antibodies at 37°C for 60 min, washed three times with PBS containing 1% Tween 20 (PBS-T), and incubated with BSA-PBS containing AF 488-conjugated goat anti-rabbit immunoglobulin G and AF 594-conjugated goat anti-mouse antibodies at 37°C for 60 min. Finally, the cells were washed three times with PBS-T and observed with a FluoView FV1000 laser-scanning confocal microscope (Olympus, Tokyo, Japan).

RESULTS

VAP-C interacts with neither VAP-A nor VAP-B. The length of VAP-A was originally reported to be 242 amino acids but was recently corrected to 249 amino acids in the GenBank database due to the detection of 7 extra amino acids in the N terminus (Fig. 1A). VAP-C is a splicing variant of VAP-B that shares the N-terminal half of the MSP domain with VAP-B but lacks the coiled-coil motif and TM region (Fig. 1A). The region spanning residues 71 to 99 of VAP-C exhibits no homology to VAP-A and VAP-B, due to the frameshift. VAP-A and VAP-B form homo- or heterodimers via their TM domains, which is required for HCV replication (9, 44). To examine whether VAP-C is capable of interacting with VAP-A and VAP-B, FLAG-tagged VAP-A, -B, or -C was coexpressed with EE-tagged VAP-A or -B in 293T cells and was immunoprecipitated with the anti-FLAG antibody. Although EE-tagged VAP-A and VAP-B were coprecipitated with FLAG-tagged VAP-B and VAP-A, as reported previously, FLAG–VAP-C was precipitated with neither EE–VAP-A nor EE–VAP-B (Fig. 1B). These results indicate that VAP-C does not interact with VAP-A and VAP-B.

VAP-C binds to NS5B and interrupts the interaction of VAP-A and VAP-B with NS5B. VAP-A and VAP-B were identified as NS5A-binding proteins by yeast two-hybrid screening (9, 44). The coiled-coil domains of VAP-A and VAP-B were involved in the binding to NS5A, contributing to the efficiency of HCV replication (9, 44). However, VAP-C does not have the coiled-coil domain (Fig. 1A) and, therefore, VAP-C was expected not to interact with NS5A. To examine whether or not interaction between VAP-C and NS5A actually occurred, HA-tagged NS5A was coexpressed with FLAG-tagged VAP-A, -B, or -C in 293T cells and was immunoprecipitated with anti-HA antibody (Fig. 2). The results showed that the expression level of FLAG–VAP-C in the transfected cells was comparable to that of FLAG–VAP-A or FLAG–VAP-B (Fig. 2A, left). Although FLAG-tagged VAP-A and VAP-B were coprecipitated with HA-NS5A, no precipitation of FLAG–VAP-C with NS5A was detected (Fig. 2A, right), indicating that VAP-C does not interact with NS5A.

The RNA-dependent RNA polymerase NS5B was shown to interact with VAP-A through the MSP domain (44). The region spanning residues 1 to 70 of VAP-C is the same as the N-terminal-half region of the MSP domain of VAP-B and exhibits 77% homology to that of VAP-A (Fig. 1A). To exam-

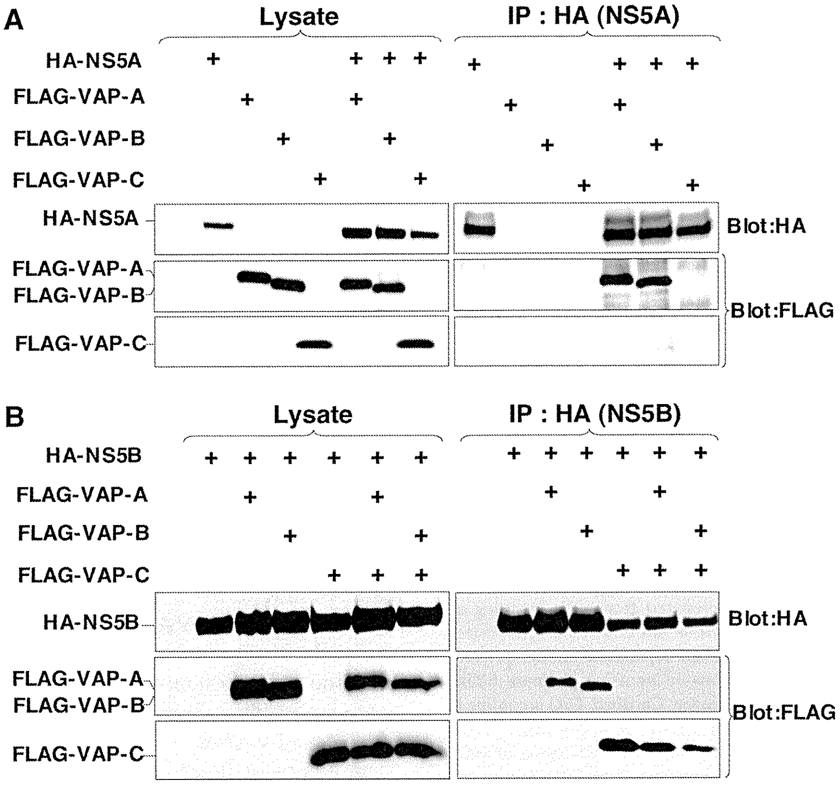

FIG. 2. VAP-C binds to NS5B but not NS5A and interrupts the interaction of VAP-A and VAP-B with NS5B. (A) The expression plasmids encoding NS5A or VAP proteins (1 μg each) were transfected into 293T cells after adjusting the total amounts of DNA to 2.0 μg with empty plasmid. HA-tagged NS5A was coexpressed with either FLAG-tagged VAP-A, VAP-B, or VAP-C in 293T cells and immunoprecipitated (IP) with anti-HA antibody, and the resulting precipitates were immunoblotted using anti-FLAG or anti-HA antibody. (B) The expression plasmids encoding NS5B or VAP proteins (1 μg each) were transfected into 293T cells after adjusting the total amounts of DNA to 3.0 μg with empty plasmid. HA-tagged NS5B was coexpressed with either FLAG-tagged VAP-A or VAP-B in the presence or absence of FLAG-tagged VAP-C in 293T cells and immunoprecipitated (IP) with anti-HA antibody, and the resulting precipitates were immunoblotted using anti-FLAG or anti-HA antibody. One percent of the lysate was used as an input control. The data in each panel are representative of the results of three independent experiments. +, present.

ine whether VAP-C is capable of interacting with NS5B, as are VAP-A and VAP-B, HA-NS5B was coexpressed with FLAG–VAP-A, FLAG–VAP-B, or FLAG–VAP-C in 293T cells and was immunoprecipitated with anti-HA antibody (Fig. 2B). Although substantial amounts of FLAG-tagged VAP-A, VAP-B, and VAP-C were coexpressed, and although all three were coprecipitated with HA-NS5B at comparable levels, the interaction of HA-NS5B with FLAG-tagged VAP-A or VAP-B was impaired by the coexpression of VAP-C, while FLAG–VAP-C was coprecipitated with HA-NS5B instead of FLAG-tagged VAP-A or VAP-B. These results suggest that VAP-C is capable of binding to NS5B and that the expression of VAP-C interrupts the interactions of NS5B with VAP-A and VAP-B.

Expression of VAP-C impairs the replication of HCV. VAP-A and VAP-B are known to support the replication of HCV RNA (2, 7). To examine the effect of VAP-C on the replication of HCV, FLAG–VAP-C was expressed in HCV replicon cells, Huh 9-13, in which a subgenomic HCV RNA of the genotype 1b strain Con1 was autonomously replicating. Huh 9-13 cells transfected with a plasmid encoding FLAG–VAP-C were harvested periodically up to 72 h posttransfection. The levels of replication of viral RNA and expression of NS5A were determined by real-time PCR and immunoblotting, respectively (Fig. 3). The expression of VAP-C reduced the intracellular RNA of the subgenomic HCV replicon in accordance with the incubation period after transfection with the expression plasmid of FLAG–VAP-C; the empty plasmid did not reduce the intracellular RNA (Fig. 3A). The expression of NS5A was gradually decreased and was undetectable at 72 h posttransfection, in contrast to the increase of VAP-C expression (Fig. 3B).

Next, to determine the effects of VAP-C expression on the replication of HCV, Huh 9-13 cells were transfected with 0 to 4 μg of the expression plasmid encoding VAP-A, VAP-B, or VAP-C and the replication of the subgenomic HCV RNA was determined at 48 h posttransfection. Although the HCV replicon cells transfected with 4 μg of a plasmid encoding FLAG–VAP-B exhibited enhancement of the RNA replication, those transfected with an equivalent amount of plasmid encoding FLAG–VAP-A or empty vector showed a slight reduction of HCV RNA replication. In contrast, the replicon cells transfected with a plasmid encoding FLAG–VAP-C exhibited a clear reduction of the HCV RNA replication in a dose-dependent manner (Fig. 3C). The expression of FLAG-tagged VAP-A, VAP-B, or VAP-C in the replicon cells was increased in correspondence with the amount of the transfected plasmid

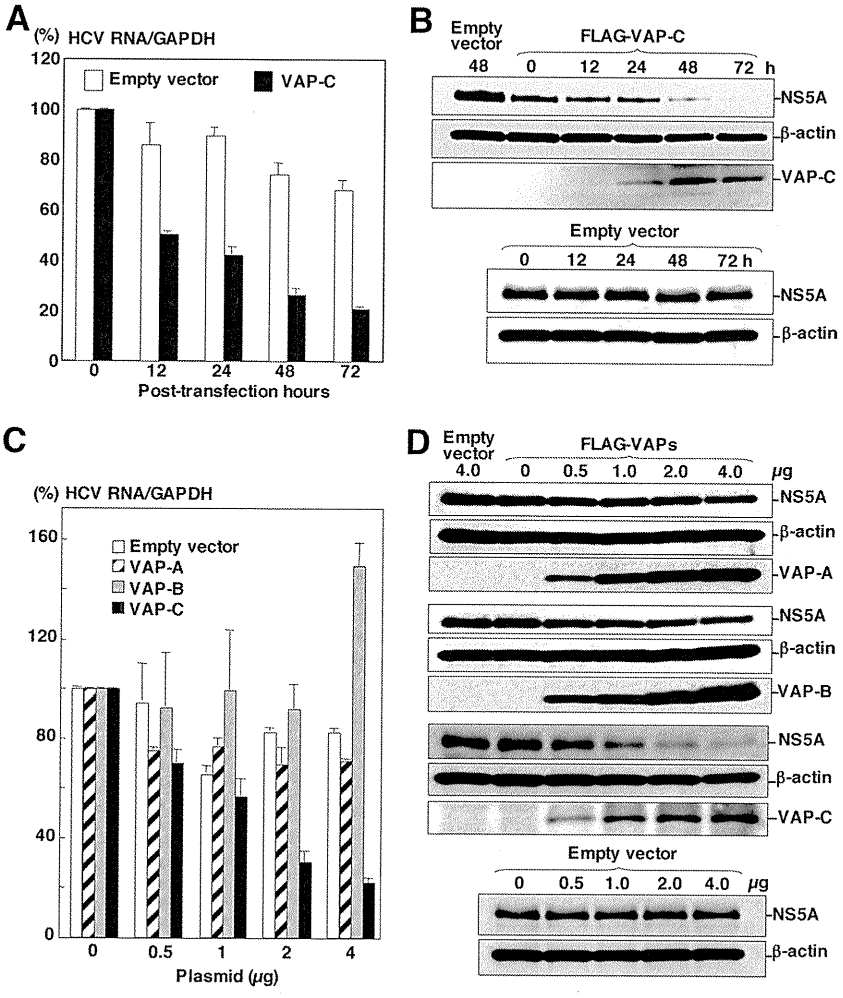

FIG. 3. Expression of VAP-C impairs the replication of HCV. (A) HCV replicon cells (Huh 9-13) were transfected with 4 μg of the expression plasmids encoding FLAG-tagged VAP-C or empty vector, and the level of intracellular HCV RNA was determined at 0, 12, 24, 48, or 72 h posttransfection by real-time PCR after normalization with GAPDH mRNA. The value of HCV RNA at 0 h posttransfection in the cell line transfected with the empty plasmid is represented as 100%. Data in this panel are shown as means ± standard deviations. (B) Huh 9-13 cells were transfected with 4 μg of the plasmid encoding FLAG-tagged VAP-C or empty plasmid, and the levels of expression of NS5A, β-actin, and VAP-C were determined at 0, 12, 24, 48, or 72 h posttransfection by immunoblotting using anti-NS5A, anti-β-actin, or anti-FLAG tag antibody. (C) Huh 9-13 cells were transfected with 0 to 4 μg of the plasmids encoding FLAG-tagged VAP-A, VAP-B, or VAP-C or empty vector, and the level of intracellular HCV RNA was determined at 72 h posttransfection as described for panel A. Data in this panel are shown as means ± standard deviations. (D) Huh 9-13 cells treated as described for panel C were harvested at 72 h posttransfection, and the levels of expression of NS5A, β-actin, VAP-A, VAP-B, and VAP-C were determined by immunoblotting. The data in each panel are representative of the results of three independent experiments.

(Fig. 3D), and the expression of NS5A was suppressed in accordance with the expression of FLAG–VAP-C, whereas the expression of FLAG–VAP-A and FLAG–VAP-B exhibited no effect on the expression of NS5A. These results suggest that the expression of VAP-C impairs the replication of HCV RNA.

VAP-C exhibits no effect on the IRES-dependent translation. The expression of VAP-C was shown to suppress the replication of the HCV RNA replication of the replicon cells. Next, to determine the effect of VAPs on the translation of HCV RNA, the reporter plasmid encoding the *Renilla* luciferase gene under the control of the CMV promoter and the firefly luciferase gene under the IRES of HCV, PV, or EMCV, in that order, was prepared as shown in Fig. 4. These reporter plasmids were introduced into Huh7OK1 cells 24 h after transfection of the expression plasmids encoding VAP-A, VAP-B, or VAP-C and harvested at 48 h posttransfection, and then the RLUs were determined. Although VAP-C exhibited a slight increase in the IRES-dependent translations of the HCV strains Con1 and JFH1, no significant effect of the expression of the VAPs on the HCV IRES-dependent translation was observed (Fig. 4A). Similarly, the expression of each of the VAPs in Huh7OK1 cells exhibited no significant effect on the IRES-dependent translation of PV or EMCV (Fig. 4B). These results indicate that the suppression of HCV RNA replication by the expression of

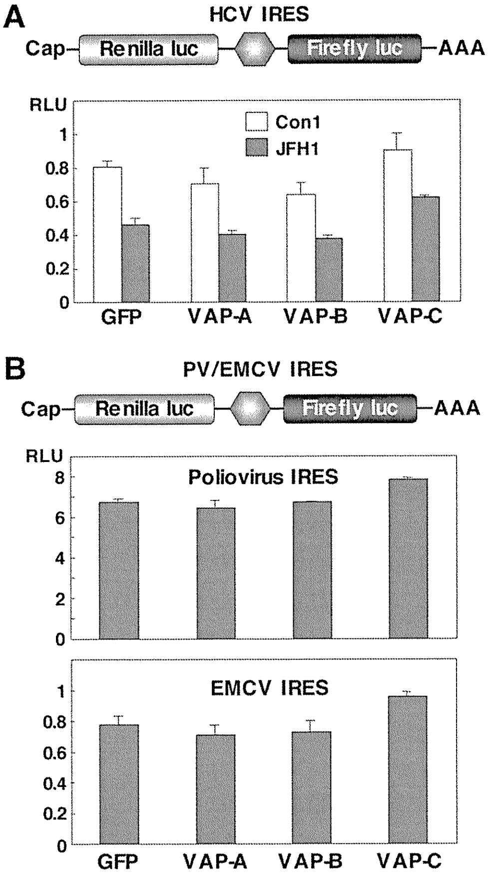

FIG. 4. VAP-C exhibits no effect on the viral IRES-dependent translation. (A) Top: structure of a reporter plasmid encoding the *Renilla* luciferase gene under the control of the CMV promoter and the firefly luciferase gene under the HCV IRES, in order. Bottom: the reporter plasmid was introduced into Huh7OK1 cells 24 h after transfection of the expression plasmids encoding VAP-A, VAP-B, or VAP-C, the cells harvested at 48 h posttransfection, and the RLUs determined after standardization with the expression of *Renilla* luciferase. (B) Top: structure of a reporter plasmid encoding the *Renilla* luciferase gene under the control of the CMV promoter and the firefly luciferase gene under the PV or EMCV IRES, in order. Bottom: each of the reporter plasmids was introduced into Huh7OK1 cells, and the RLU values were determined as described for panel A. Data in this figure are shown as the means ± standard deviations.

VAP-C was not due to the suppression of the IRES-dependent translation of the viral RNA genome.

VAP-C impairs HCV propagation. To examine the effect of VAP expression on HCV propagation, Huh7OK1 cells transfected with the expression plasmids encoding VAP-A, VAP-B, or VAP-C were infected with JFH1 virus, and the levels of production of the viral RNA, core protein, and infectious particles were determined at 96 h postinfection. The production of intracellular and extracellular viral RNA was increased up to 10 to 30 times and 2 to 3 times, respectively, by the expression of VAP-A or VAP-B whereas it was clearly decreased in a dose-dependent manner by the expression of VAP-C (Fig. 5A). Although the extracellular core protein was increased from 0.6 to 2.6 nmol/liter by the expression of VAP-A or VAP-B, as seen in the production of viral RNA, the intracellular core protein showed only a marginal increase (40 to 65 nmol/liter) (Fig. 5A). Although the reason for the discrepancy between the intracellular production of viral RNA and core protein is not known at the moment, some mechanisms other than RNA translation might be involved, because VAP expression exhibited no effect on the HCV IRES-dependent translation, as shown in Fig. 4A. In contrast to the enhancement of core protein production by the expression of VAP-A or VAP-B, the expression of VAP-C significantly reduced both the intracellular and extracellular expression of the core protein (Fig. 5A). Furthermore, the production of infectious particles in the culture supernatants of Huh7OK1 cells infected with JFH1 virus was slightly enhanced by the expression of VAP-A or VAP-B, whereas it was suppressed by the expression of VAP-C (Fig. 5A). To further confirm the effects of VAPs on the expression of HCV proteins, Huh7OK1 cells transfected with various amounts of the expression plasmids of VAP-A, VAP-B, or VAP-C and infected with the JFH1 virus were examined by immunoblotting (Fig. 5B). Although the expression of VAP-A or VAP-B exhibited no effect on NS5A expression, VAP-C expression clearly decreased the expression of NS5A in a dose-dependent manner. These results clearly indicate that the expression of VAP-C negatively regulates HCV propagation. Overexpression of VAP-C did not affect the endogenous expression of VAP-A or VAP-B (Fig. 5C), suggesting that suppression of HCV propagation by VAP-C is not due to the reduction of VAP-A or VAP-B expression.

Lack of VAP-C expression in human livers. VAP-C consists of the first 70 amino acid residues of VAP-B and the subtype-specific 29 amino acid residues derived from frameshift (Fig. 1A). The VAP-C-specific antibody generated by immunization with the peptide corresponding to the residues from 86 to 98 clearly detected VAP-C but neither VAP-A nor VAP-B in cells transfected with expression plasmids encoding FLAG-tagged VAP-A, VAP-B, or VAP-C (Fig. 6A). To determine the distribution of VAPs in human organs, the pool lysates of various organs prepared from several people were examined by immunoblotting (Fig. 6B). Expression of VAP-A was detected clearly in the kidney, lung, prostate, and liver; slightly in the duodenum, uterus, vagina, and bladder; and barely in the small intestine and stomach. VAP-B was detected clearly in the bladder, kidney, and prostate and slightly in the duodenum, small intestine, uterus, vagina, and liver. Expression of VAP-C was detected clearly in the stomach, uterus, kidney, and bladder; slightly in the duodenum, small intestine, and prostate; and barely detected in the vagina, lung, and liver. Several bands smaller than the expected size of VAP-C were observed in the stomach, duodenum, small intestine, uterus, vagina, prostate, and bladder. Because the main target of HCV replication is thought to be the liver, we next examined the expression of VAPs in individual human liver samples. VAP-A and VAP-B were clearly detected in the liver tissues obtained from chronic hepatitis C patients and a healthy donor, but no expression of VAP-C was detected (Fig. 6C). These results suggest that the expression of VAP-C may participate in the determination of tissue tropism of HCV propagation.

Substitution of Ser for Pro^{56} in VAPs leads to suppression of HCV replication. A single mutation of Pro^{56} to Ser (P56S) of VAP-B has been reported to be highly associated with amyotrophic lateral sclerosis (ALS), and the P56S mutation of VAP-B but not of VAP-A has been shown to induce large

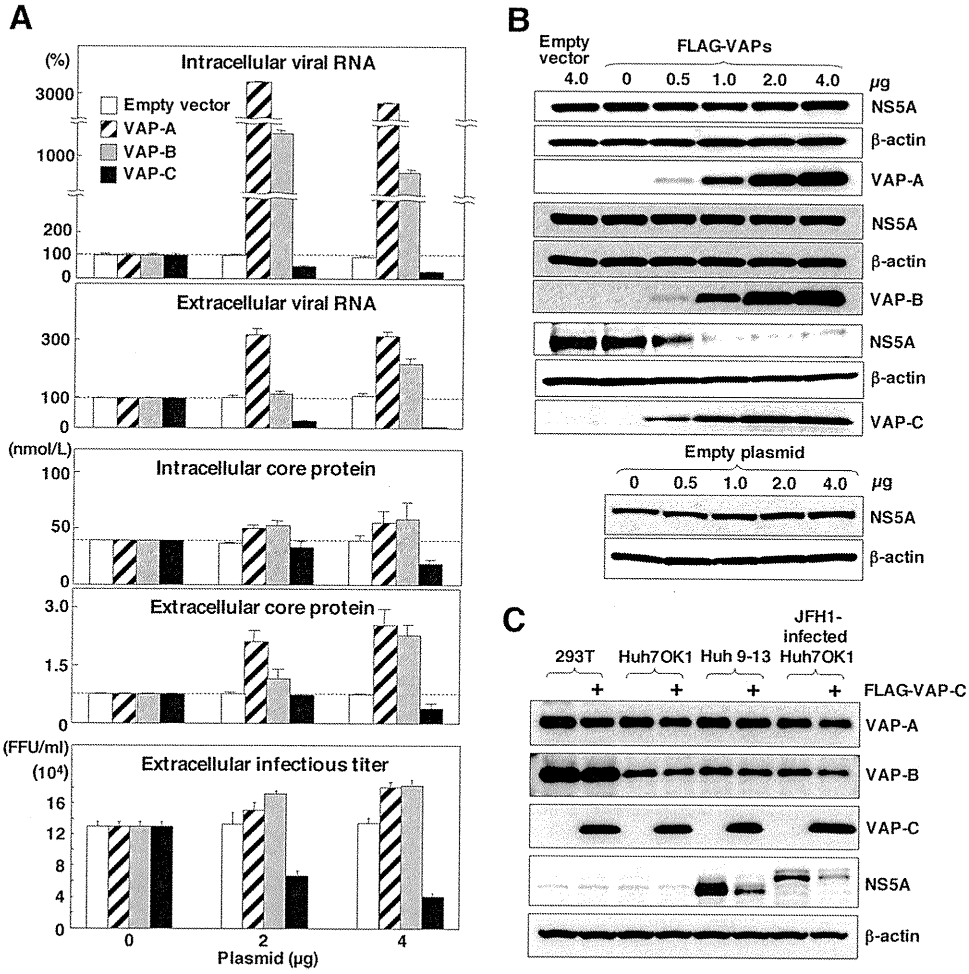

FIG. 5. VAP-C impairs HCV propagation but does not affect endogenous expression of VAP-A or VAP-B. Huh7OK1 cells transfected with 0 to 4 μg of plasmid encoding the FLAG-tagged VAP-A, VAP-B, or VAP-C or empty vector were infected with strain JFH1 at an MOI of 0.05 at 14 h posttransfection and then harvested at 96 h postinfection. (A) The intracellular and extracellular expression levels of viral RNA (top) and core protein (middle) were determined by real-time PCR and ELISA, respectively. Infectious viral titers in the culture supernatants were determined by focus-forming assay (bottom). Data in this panel are shown as the means ± standard deviations. (B) The expression levels of NS5A, β-actin, VAP-A, VAP-B, and VAP-C were determined by immunoblotting using anti-NS5A, anti-β-actin, or anti-FLAG tag antibody. (C) The embryonic kidney cell line (293T), the cured hepatoma cell line (Huh7OK1), and the replicon cell line (Huh 9-13) were transfected with 2 μg of the plasmid encoding FLAG-tagged VAP-C (+) or empty plasmid. In the case of the infected cells, Huh7OK1 cells were infected with strain JFH1 at an MOI of 0.05, reseeded onto the tissue culture plate at 96 h postinfection, and then transfected with 2 μg of the plasmids. These cells were harvested at 36 h posttransfection and examined by immunoblotting using antibodies to VAP-A, VAP-B, FLAG, NS5A, and β-actin. The data in each panel are representative of the results of three independent experiments.

aggregations of ER in culture cells and to sequester the wild-type protein into ubiquitinated inclusions (29, 37). To examine the effects on the replication of HCV of the P56S mutation in VAPs, FLAG-tagged VAP mutants were expressed in the HCV replicon cells. RNA replication of the subgenomic replicon in Huh 9-13 cells was impaired by the expression of each of the mutant VAPs (Fig. 7A, left). The expression of NS5A in the replicon cells was decreased by the expression of the mutant VAPs in a dose-dependent manner (Fig. 7A, right). Next, to examine the effect of the expression of the P56S VAP mutants on HCV propagation, Huh7OK1 cells expressing the FLAG-tagged VAP mutants were infected with JFH1 virus. The production of intracellular and extracellular viral RNA at 96 h postinfection was decreased by the expression of the P56S mutation in VAPs (Fig. 7B). Although the results of a previous study indicated that the expression of the P56S mutant of VAP-B but not that of VAP-A induced a large aggregation of ER in hamster ovary cell line CHO (37), the P56S mutants of VAP-A and VAP-B but not that of VAP-C exhibited accumulation of membranous aggregates in Huh 9-13 cells (Fig. 7C). These results indicate that the P56S mutation in both VAP-B and VAP-A induces aggregation of ER in human hepatoma cells, which in turn leads to the suppression of HCV propagation.

DISCUSSION

The replication of HCV has been shown to require several host proteins, including VAP-A/VAP-B (6, 9, 44), FBL2 (46), FKBP8 (34), hB-ind1 (40), Hsp90 (28, 34, 45), and cyclophilins